Quantification of primary and secondary organic aerosol sources by combined factor analysis of extractive electrospray ionisation and aerosol mass spectrometer measurements (EESI-TOF and AMS)

Yandong Tong[1], Lu Qi[1], Giulia Stefenelli[1], Dongyu S. Wang[1], Francesco Canonaco[1], Urs Baltensperger[1], André S.H. Prévôt[1], Jay Slowik[1,]*

[1]Laboratory of Atmospheric Chemistry, Paul Scherrer Institute (PSI), 5232 Villigen, Switzerland

*Correspondence to Jay Slowik (jay.slowik@psi.ch)

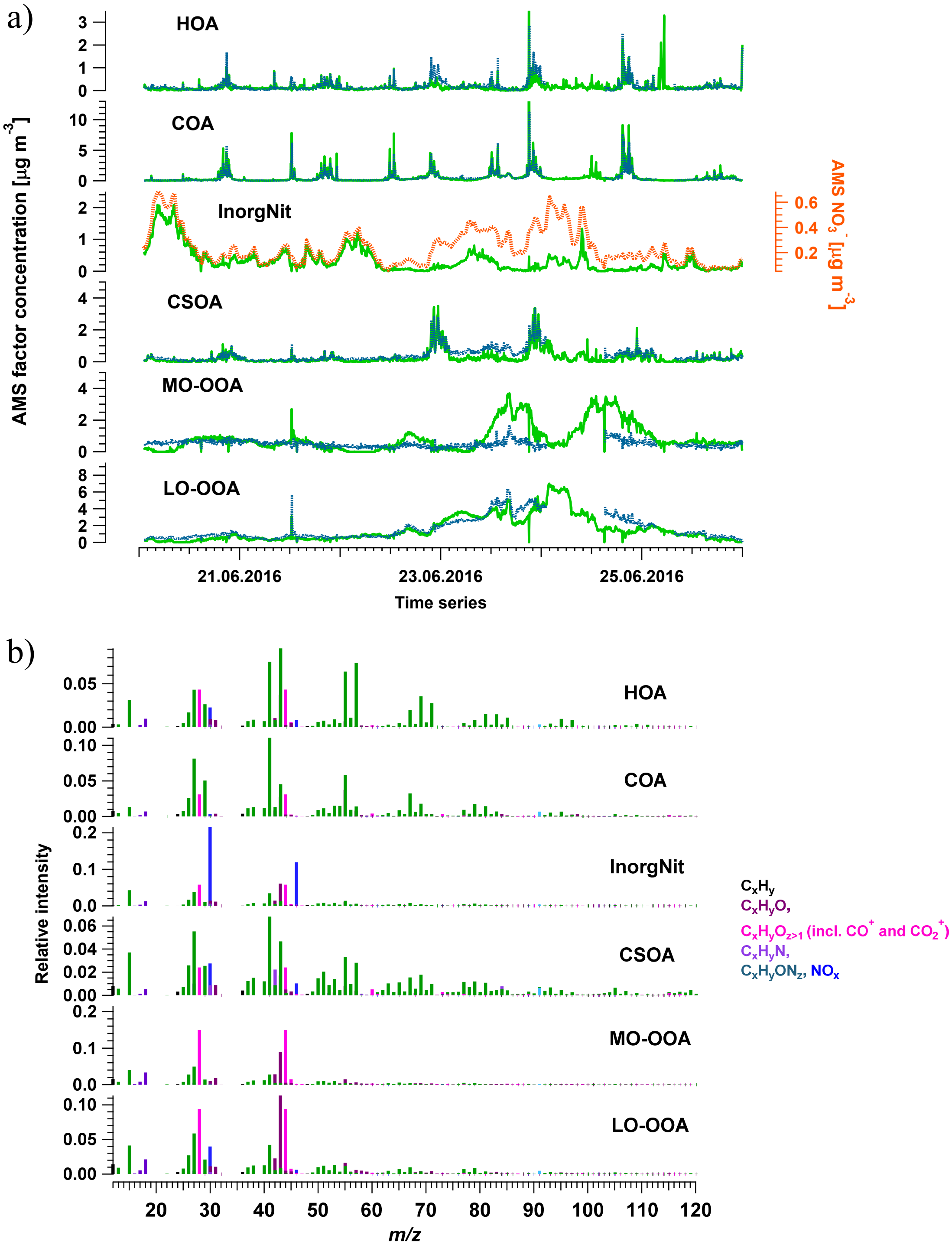

a)
HOA
COA
InorgNit
CSOA
MO-OOA
LO-OOA
AMS factor concentration [µg m-3]
AMS NO3- [µg m-3]
21.06.2016
23.06.2016
25.06.2016
Time series
b)
Relative intensity
m/z
CxHy
CxHyO,
CxHyOz>1 (incl. CO+ and CO2+)
CxHyN,
CxHyONz, NOx

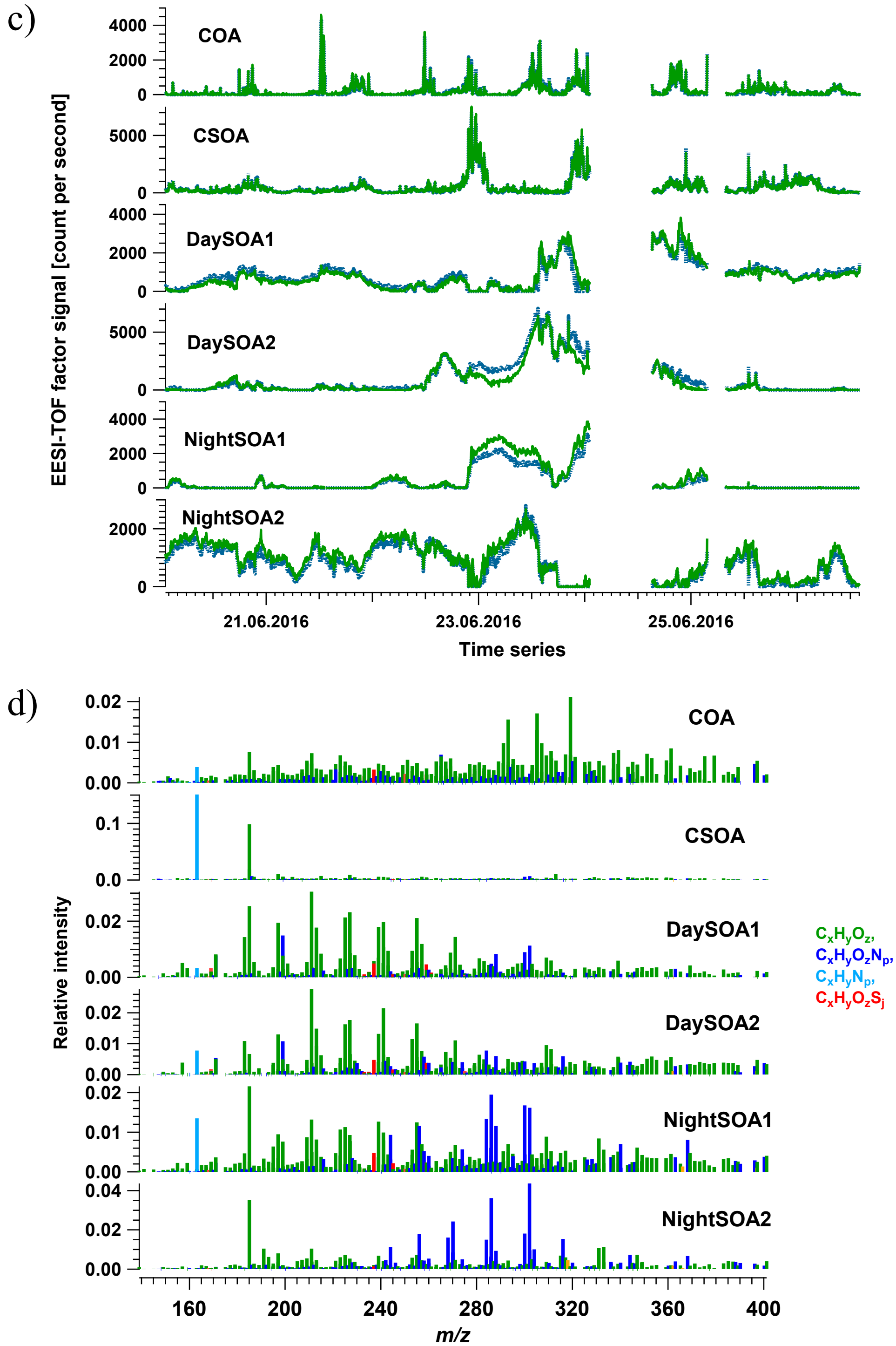

Figure S1. The time series and factor profile of AMS-only PMF solution is shown in a) and b), and the time series and factor profile of EESI-TOF-only PMF solution is shown in c) and d), respectively. Green lines are the factor time series of AMS-only and EESI-TOF-only PMF solution in this study, whereas the blue lines are the factor time series of solution in Stefenelli et al. (2019). Note, in addition to the original AMS PMF solution from Stefenelli et al. (2019), the AMS-only PMF solution from this study yields an inorganic nitrate factor (InorgNit), because NO^+ and NO_2^+ are included in the input matrix.

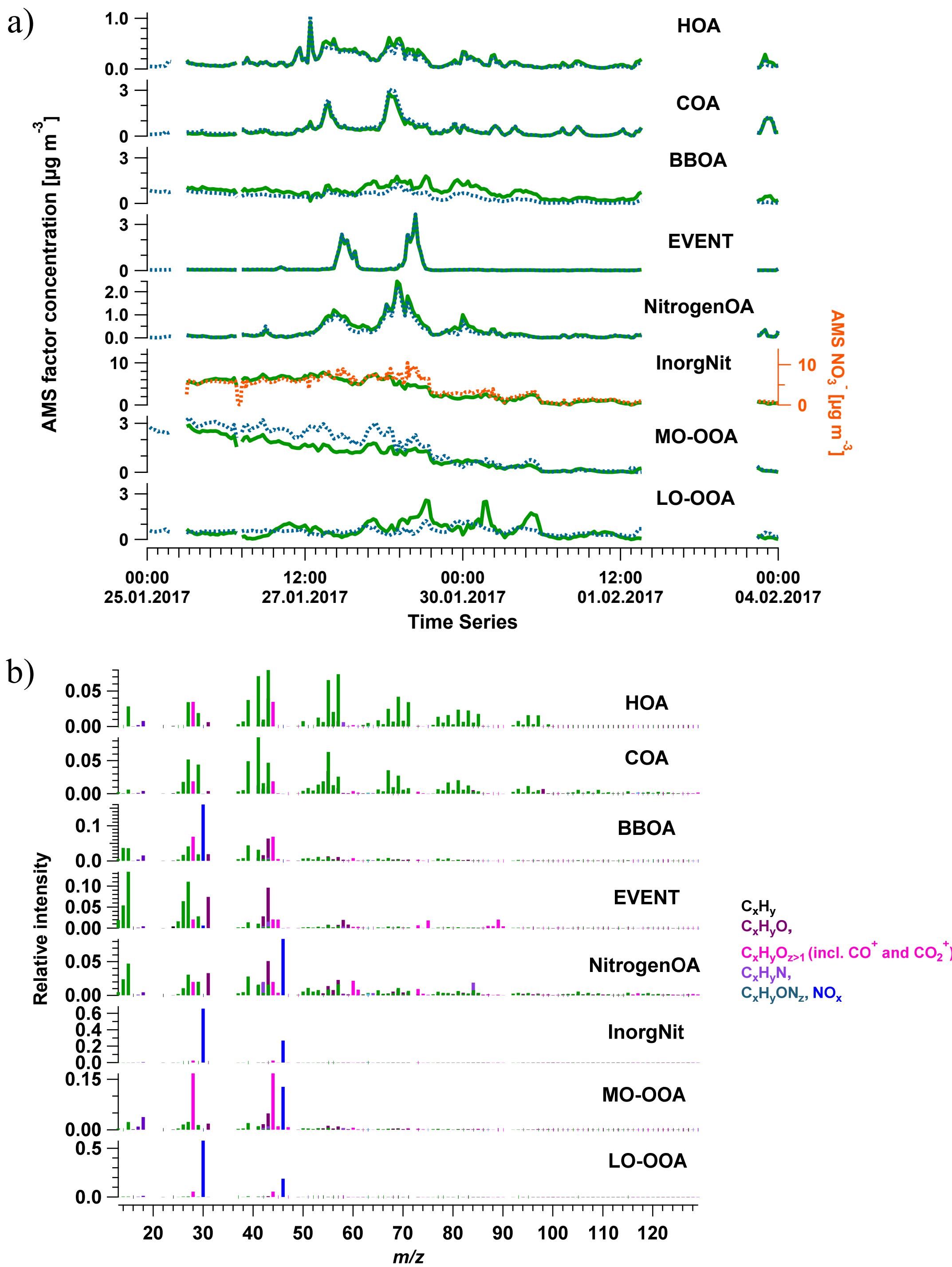
a)
HOA
COA
BBOA
EVENT
NitrogenOA
InorgNit
MO-OOA
LO-OOA
AMS factor concentration [µg m^{-3}]
AMS NO_3^- [µg m^{-3}]
00:00 25.01.2017
12:00 27.01.2017
00:00 30.01.2017
12:00 01.02.2017
00:00 04.02.2017
Time Series
b)
HOA
COA
BBOA
EVENT
NitrogenOA
InorgNit
MO-OOA
LO-OOA
Relative intensity
m/z
C_xH_y
C_xH_yO,
$C_xH_yO_{z>1}$ (incl. CO^+ and CO_2^+)
C_xH_yN,
$C_xH_yON_z$, NO_x

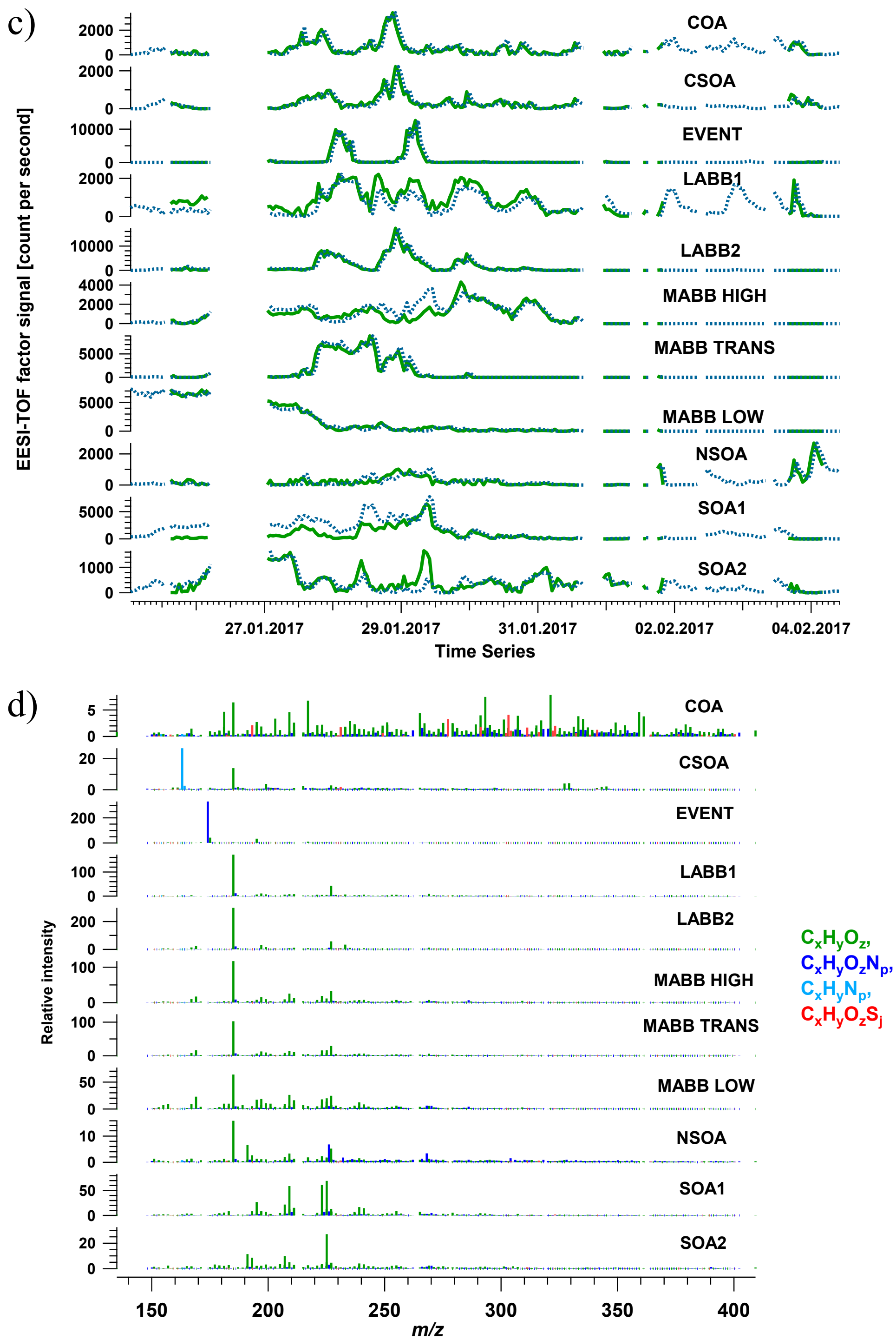

Figure S2. The time series and factor profile of AMS-only PMF solution is shown in a) and b), and the time series and factor profile of EESI-TOF-only PMF solution is shown in c) and d), respectively. Green lines are the factor time series of AMS-only and EESI-TOF-only PMF solution in this study, whereas the blue lines are the factor time series of solution in Qi et al. (2019). Note, in addition to the original AMS PMF solution from Qi et al. (2019), the AMS-only PMF solution in this study yields a inorganic nitrate factor (InorgNit), because NO^+ and NO_2^+ are included in the input matrix.

a)

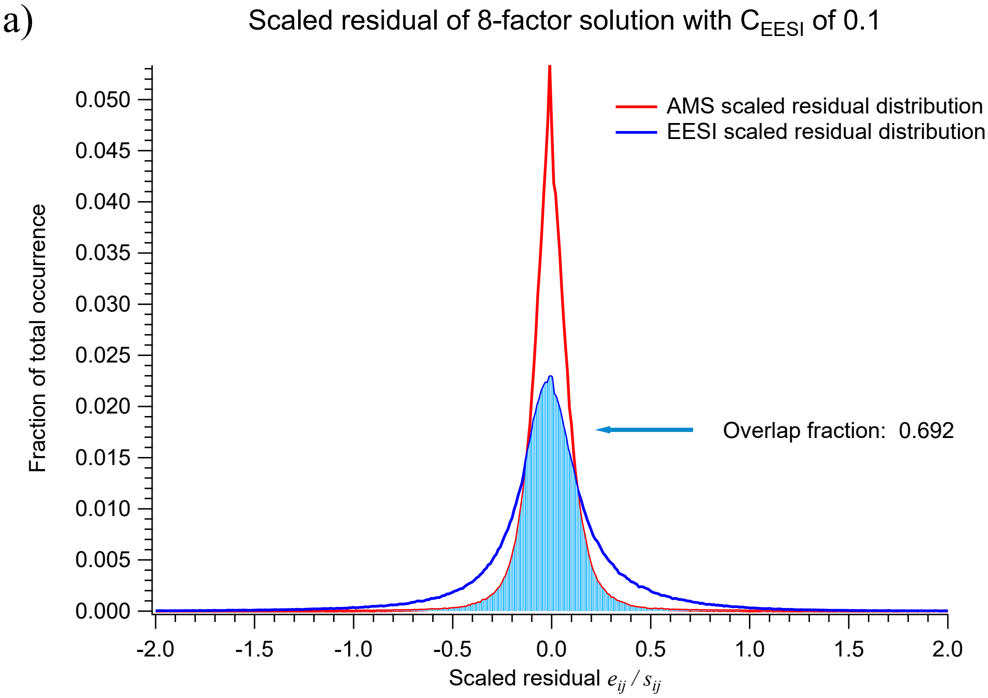

Scaled residual of 8-factor solution with C_EESI of 0.1
AMS scaled residual distribution
EESI scaled residual distribution
Overlap fraction: 0.692
Fraction of total occurrence
Scaled residual e_ij / s_ij

b)

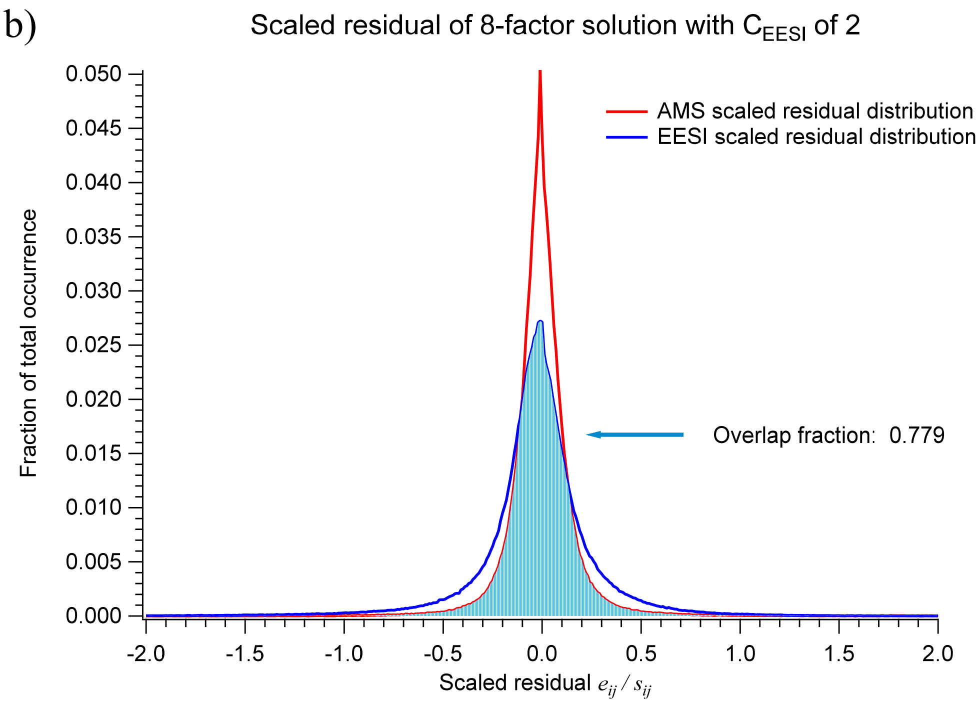

Scaled residual of 8-factor solution with C_EESI of 2
AMS scaled residual distribution
EESI scaled residual distribution
Overlap fraction: 0.779
Fraction of total occurrence
Scaled residual e_ij / s_ij

c)

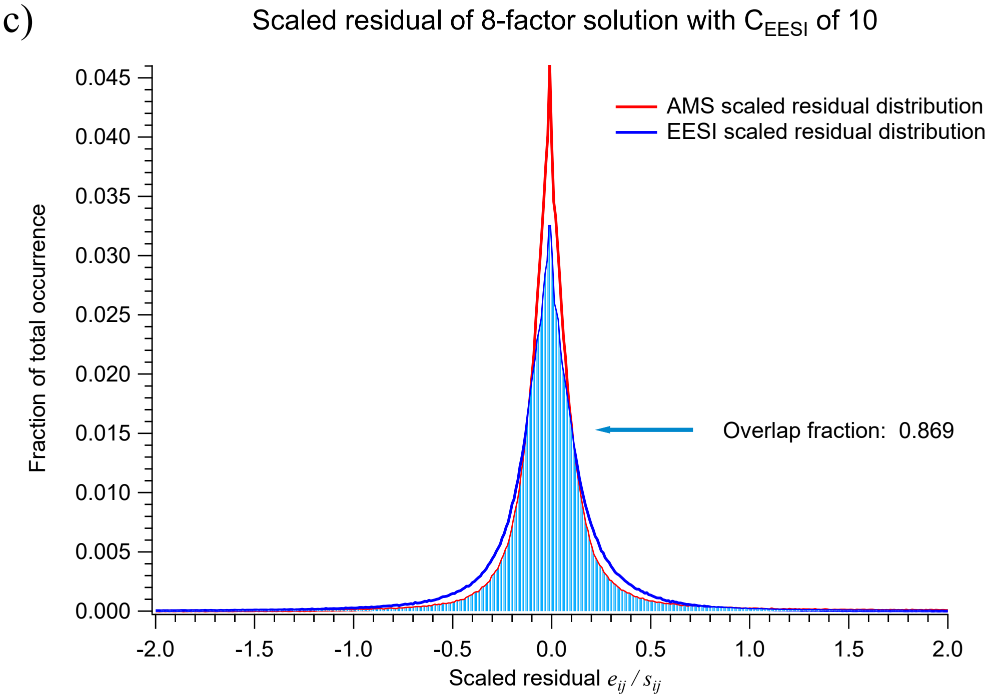

Figure S3. Scaled residual distribution of AMS (red line) and EESI (blue line) in an 8-factor solution from joint dataset in Zurich summer and corresponding overlap fractions when C_{EESI} is equal to 0.1 in a), 2 in b), and 10 in c), respectively. Balanced solution is shown in b), whereas in a) and c), AMS and EESI is overweighted, respectively.

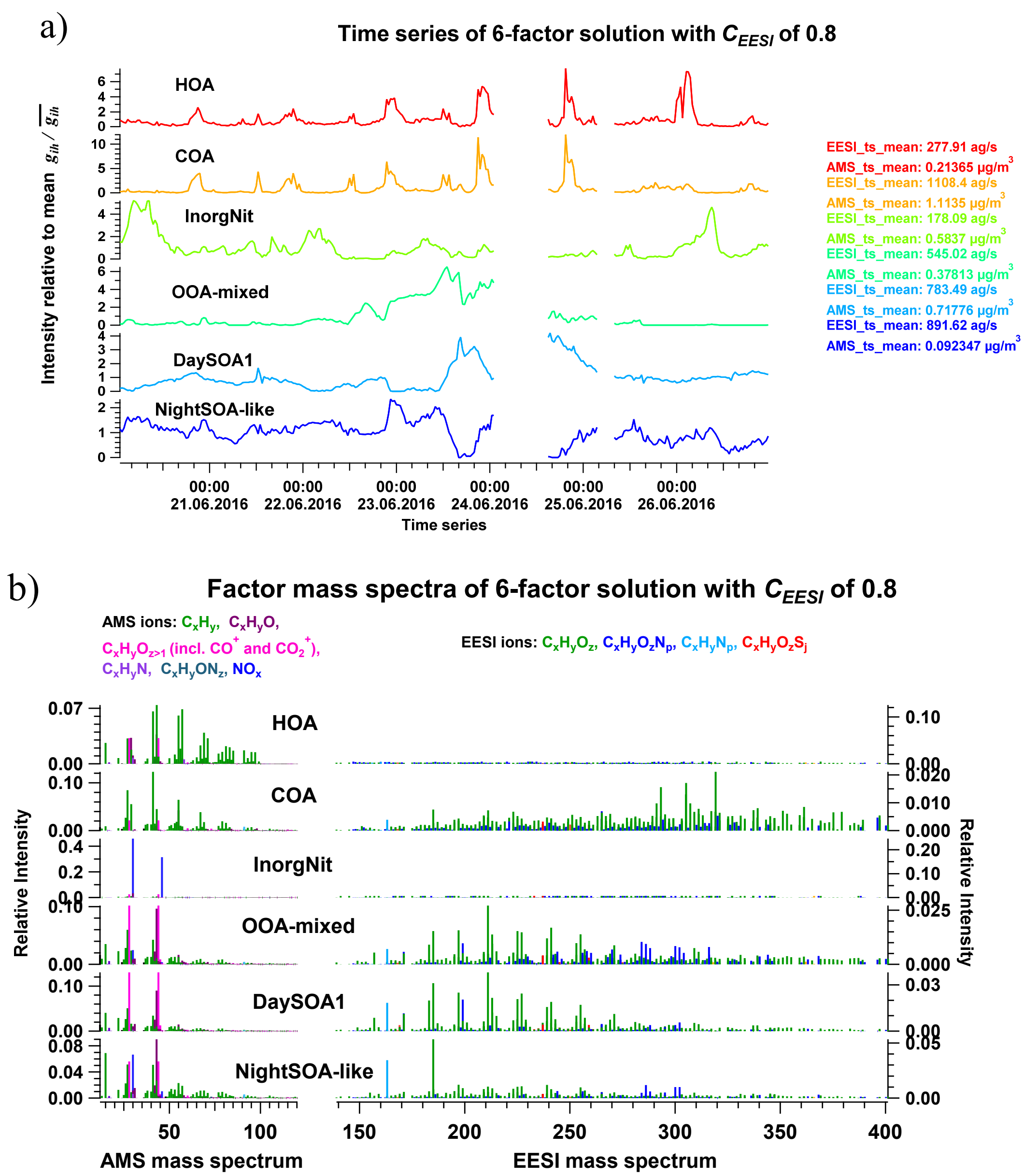

Figure S4. Factor time series in a) and mass spectra in b) for 6-factor solution with C_{EESI} of 0.8 for Zurich summer dataset.

a)

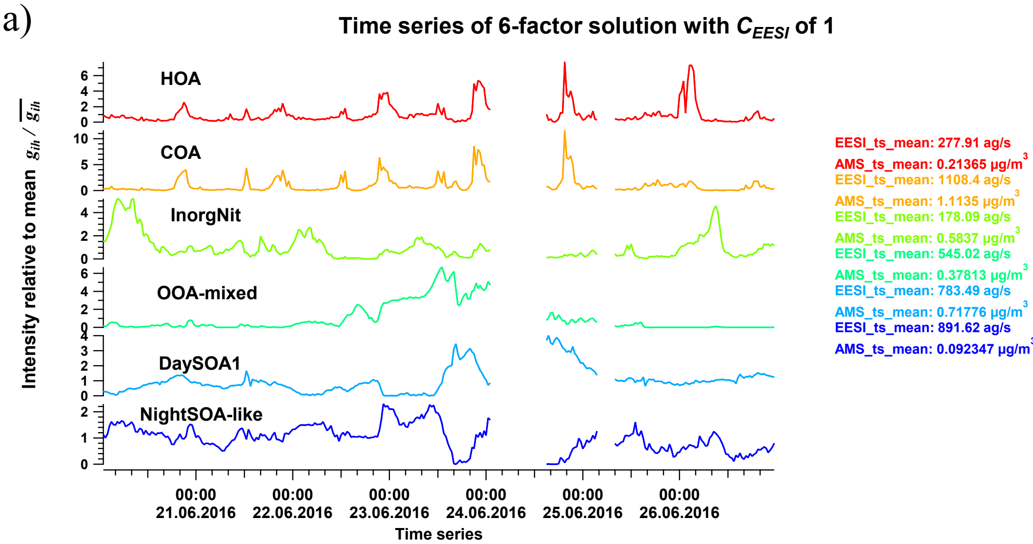

b)

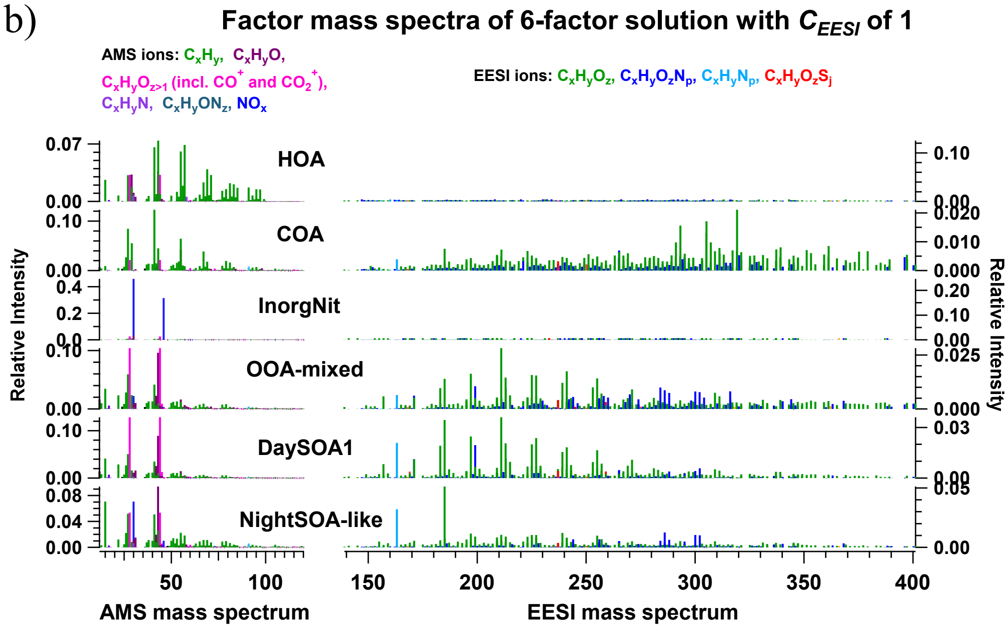

Figure S5. Factor time series in a) and mass spectra in b) for 6-factor solution with C_{EESI} of 1 for Zurich summer dataset.

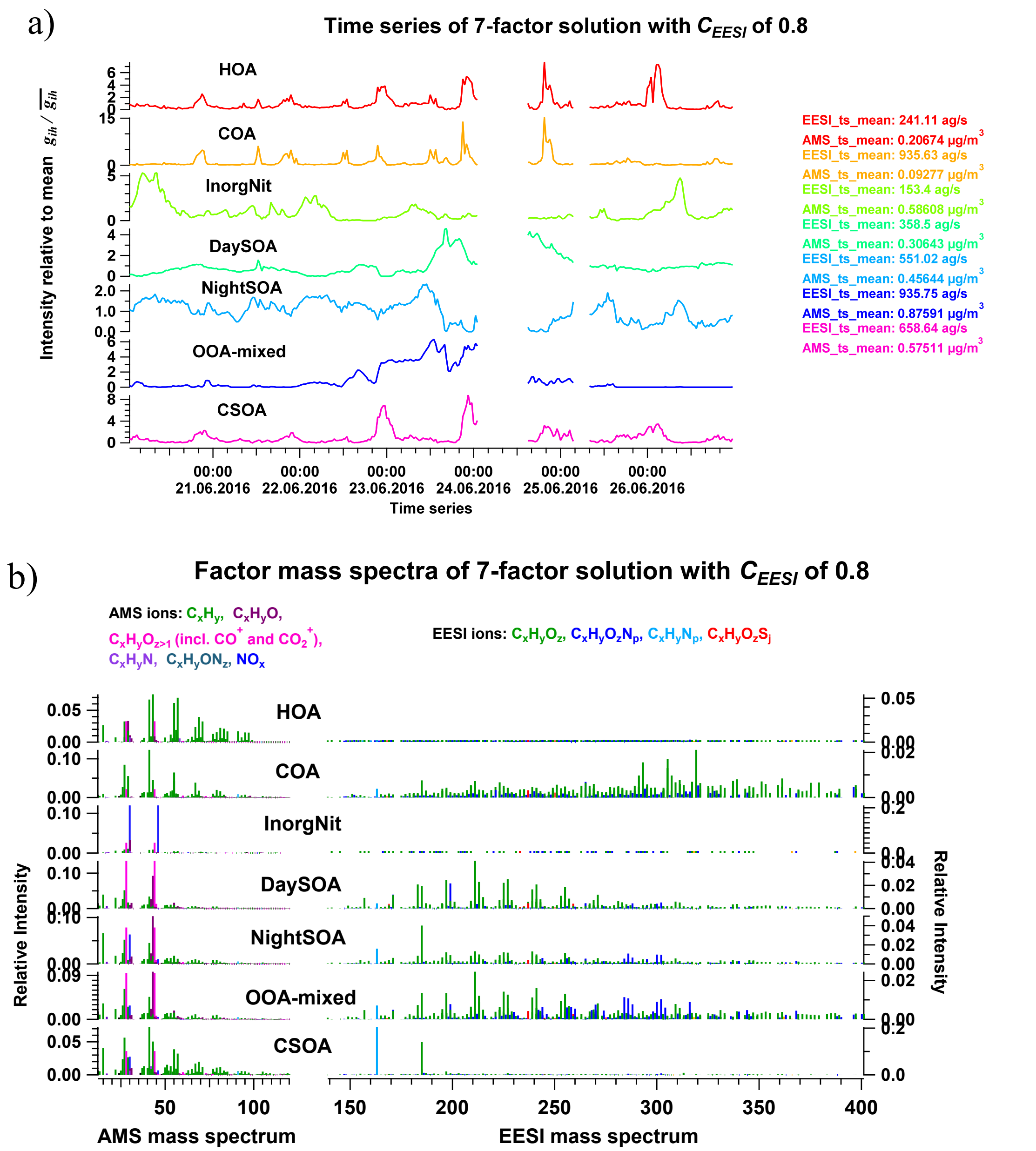

Figure S6. Factor time series in a) and mass spectra in b) for 7-factor solution with C_{EESI} of 0.8 for Zurich summer dataset.

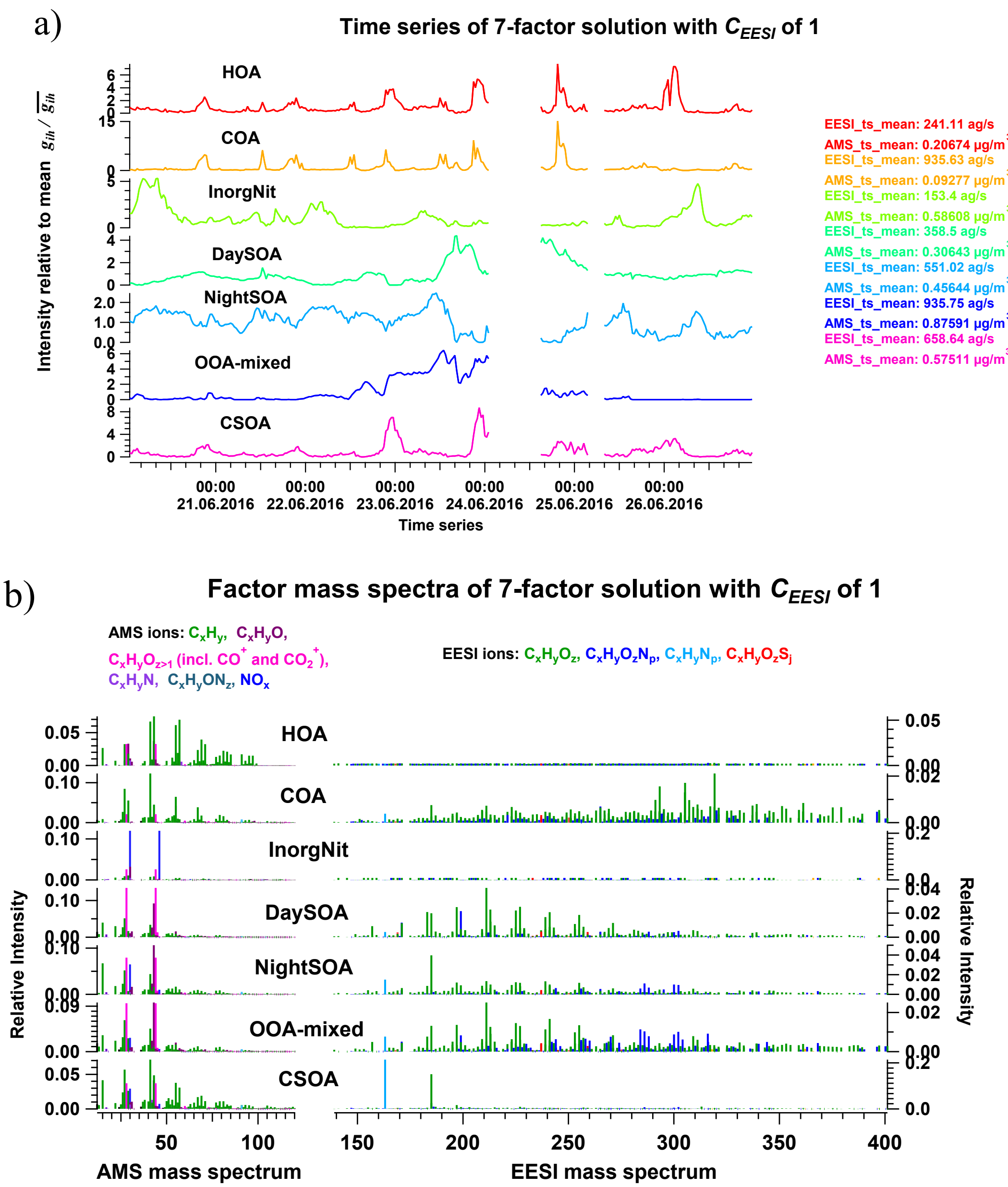

Figure S7. Factor time series in a) and mass spectra in b) for 7-factor solution with C_{EESI} of 1 for Zurich summer dataset.

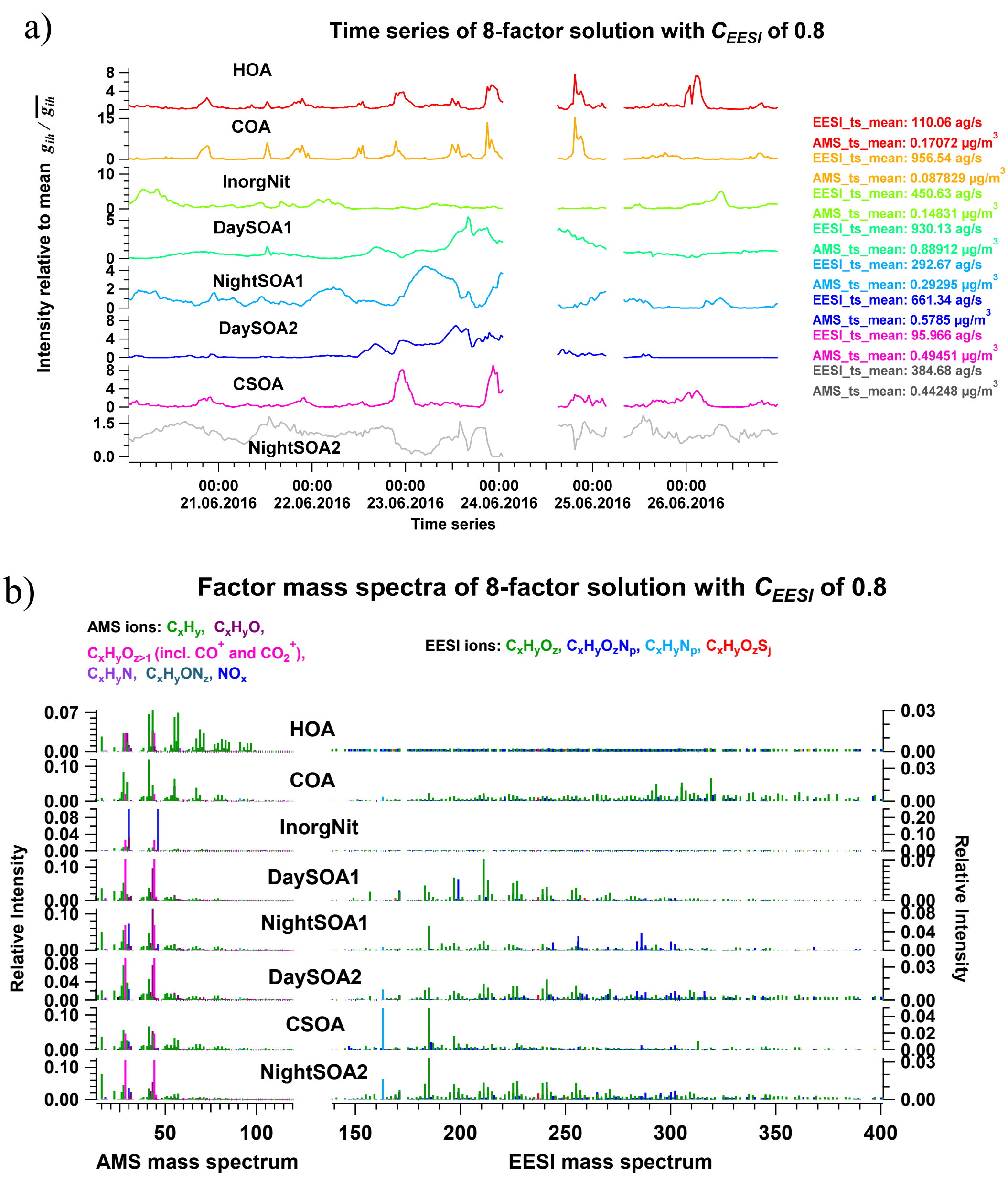

Figure S8. Factor time series in a) and mass spectra in b) for 8-factor solution with C_{EESI} of 0.8 for Zurich summer dataset.

a)

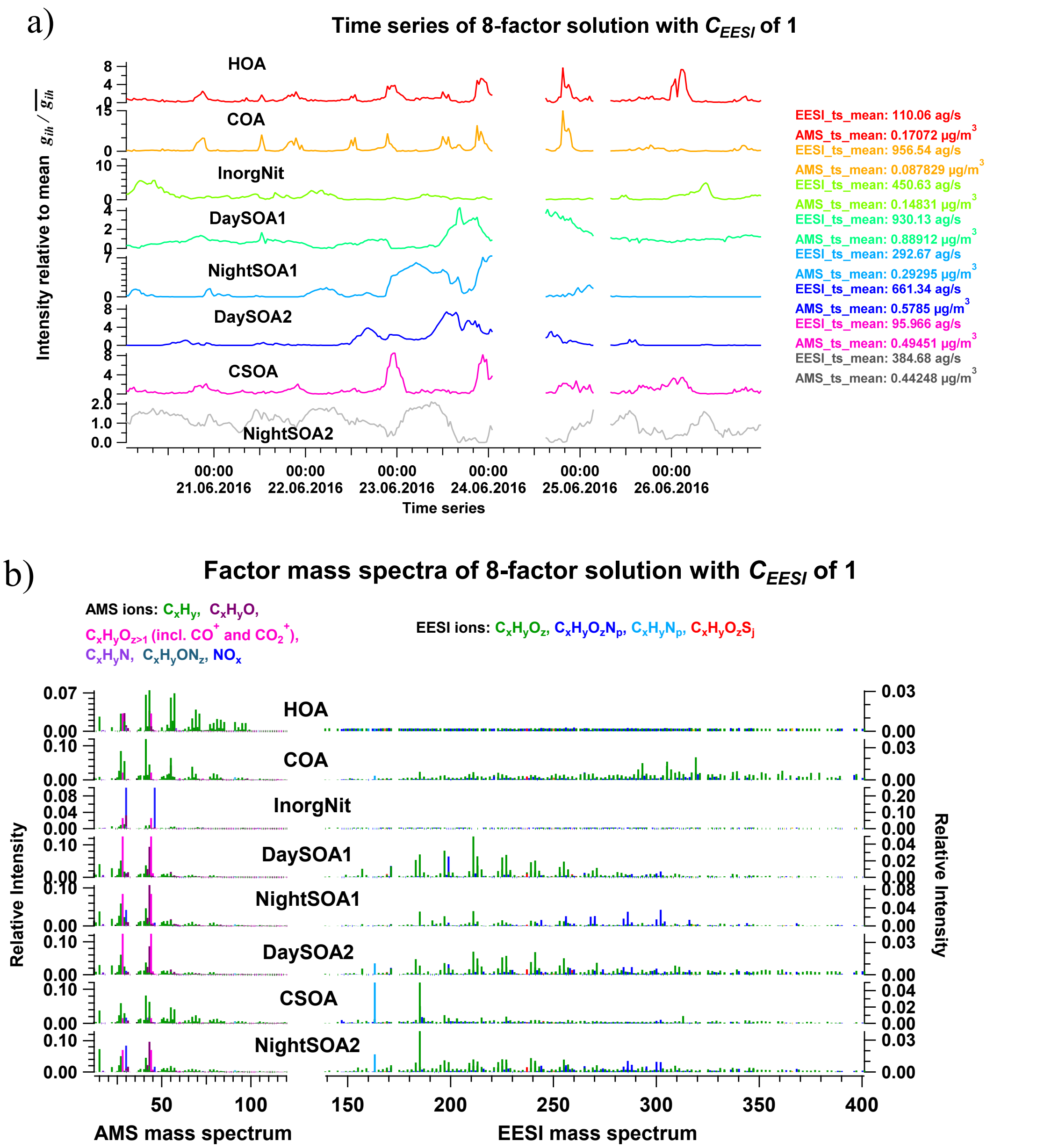

Figure S9. Factor time series in a) and mass spectra in b) for 8-factor solution with C_{EESI} of 1 for Zurich summer dataset.

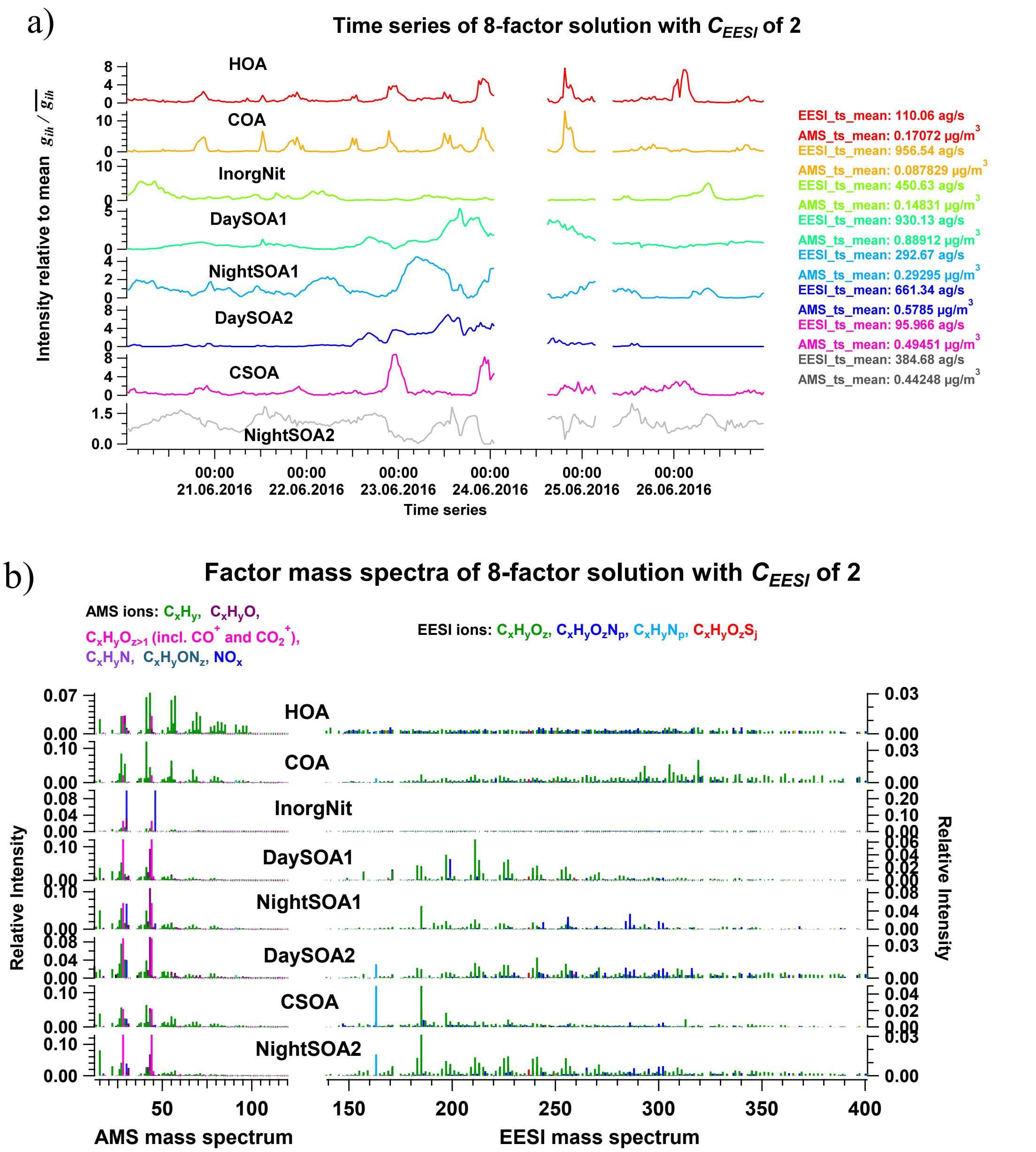

Figure S10. Factor time series in a) and mass spectra in b) for 8-factor solution with C_{EESI} of 2 for Zurich summer dataset.

a)

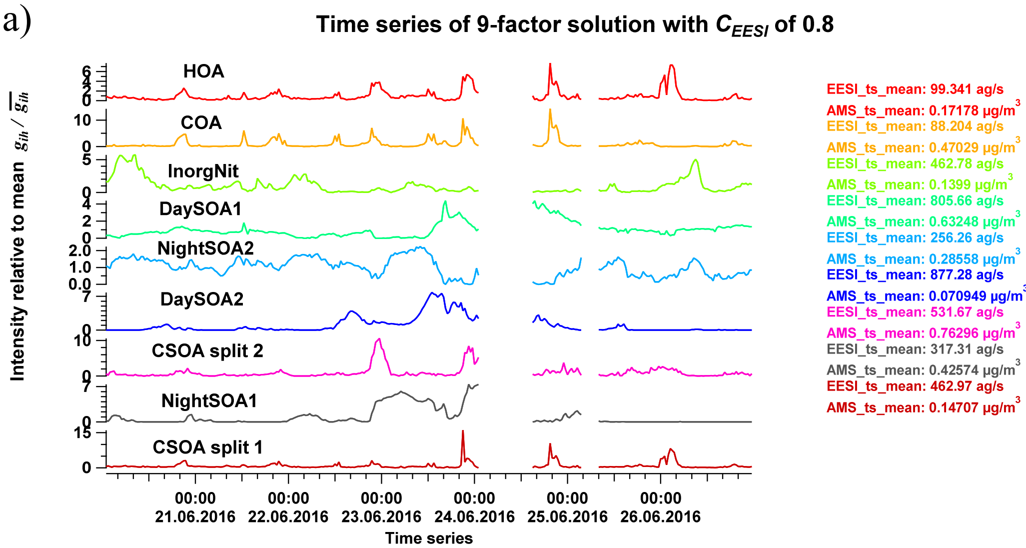

b)

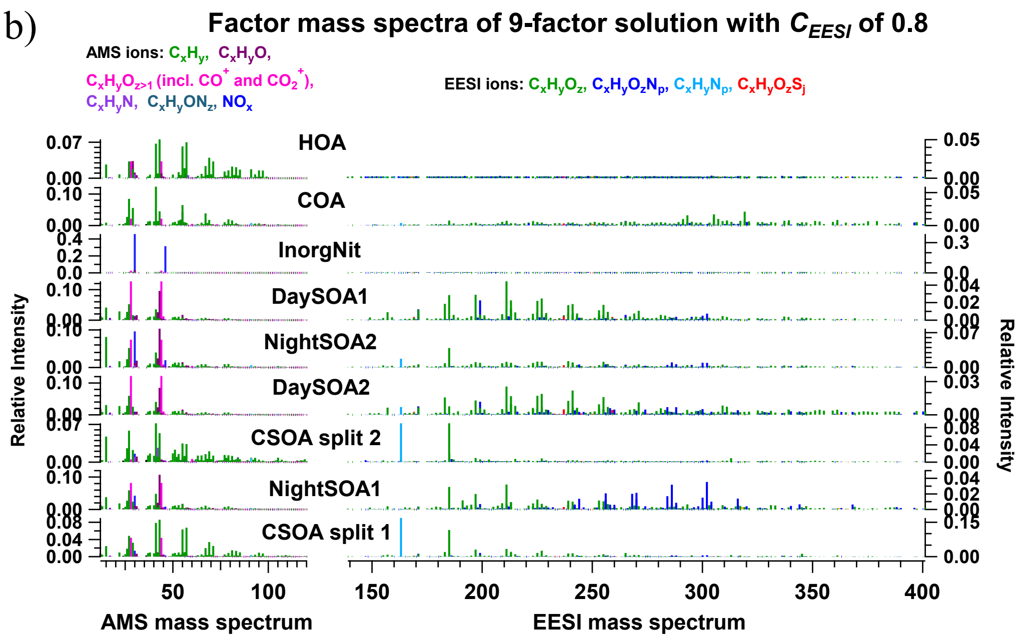

Figure S11. Factor time series in a) and mass spectra in b) for 9-factor solution with C_{EESI} of 0.8 for Zurich summer dataset.

a)

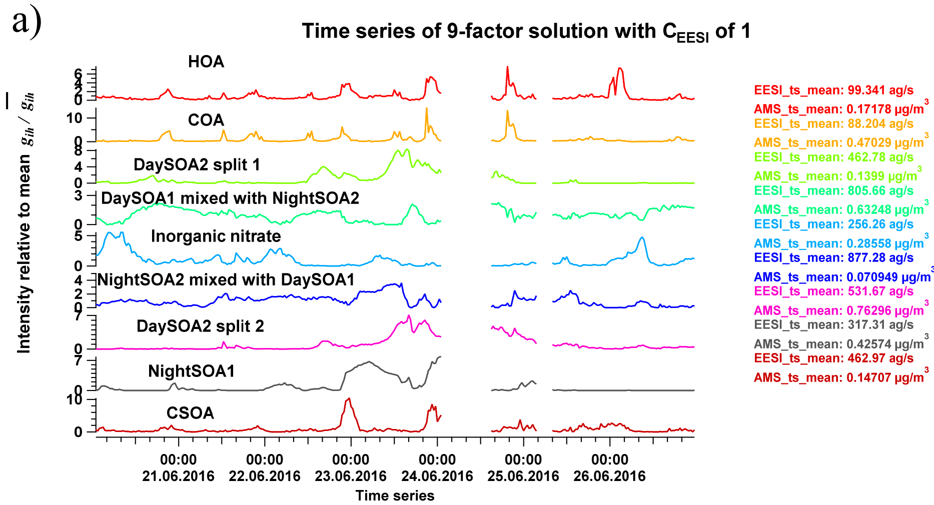

b)

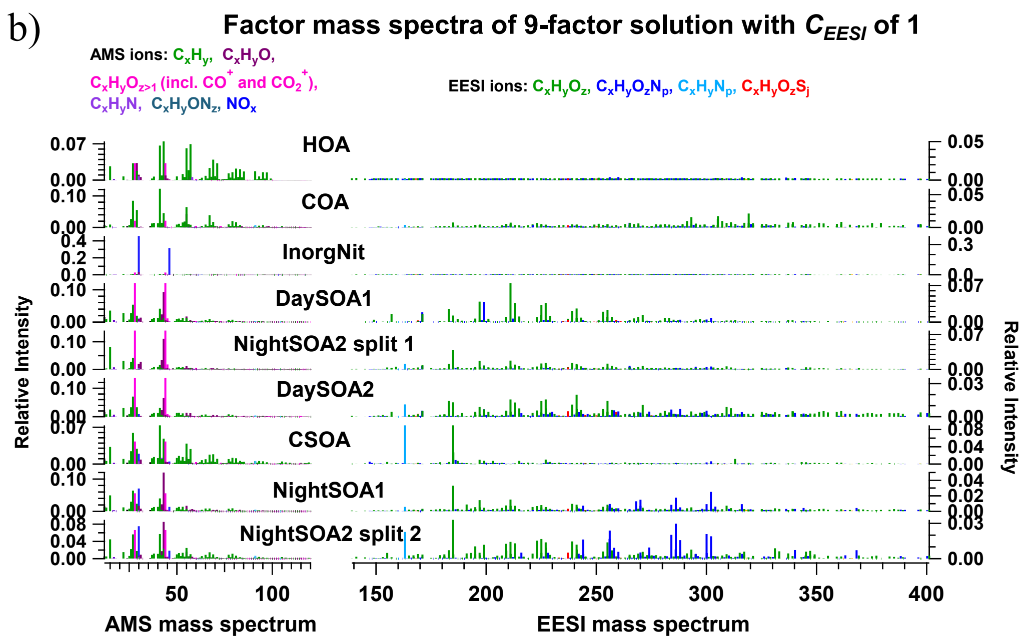

Figure S12. Factor time series in a) and mass spectra in b) for 9-factor solution with C_{EESI} of 1 for Zurich summer dataset.

a)

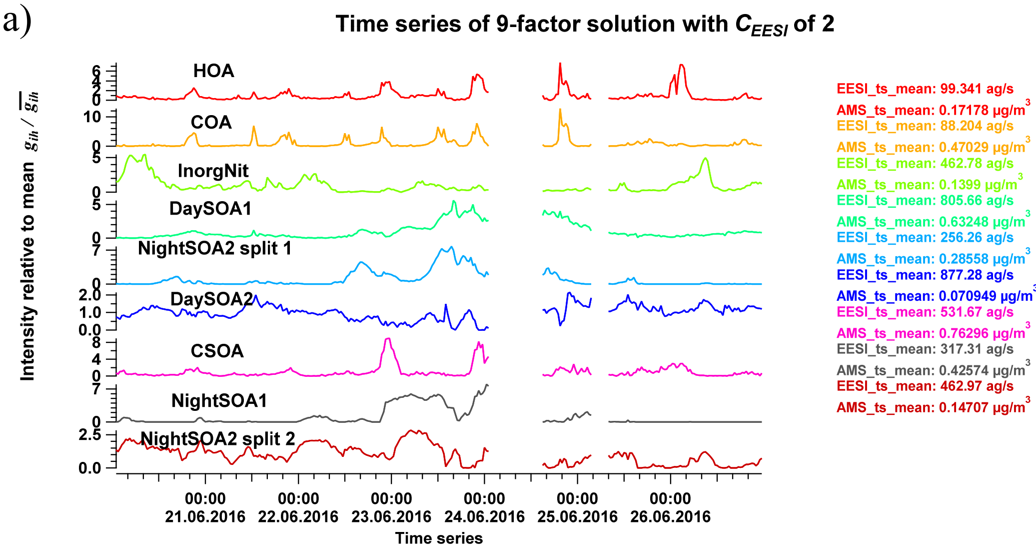

b)

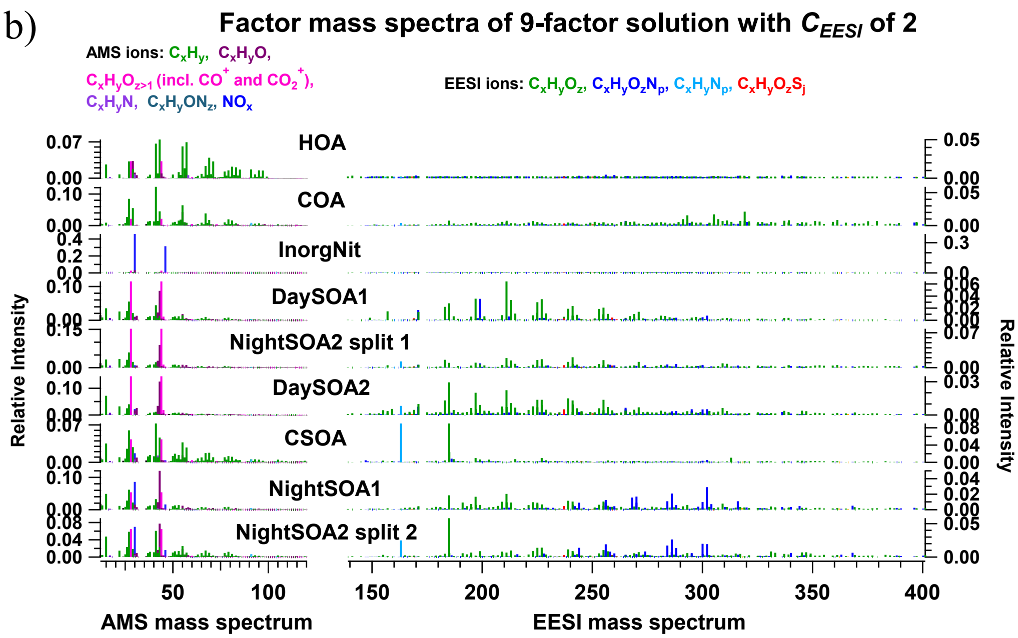

Figure S13. Factor time series in a) and mass spectra in b) for 9-factor solution with C_{EESI} of 2 for Zurich summer dataset.

a)

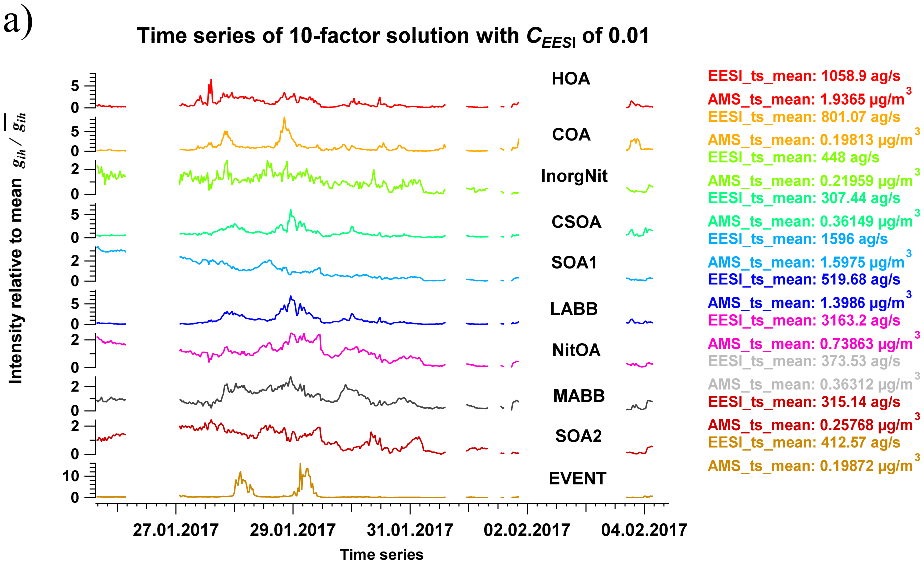

b)

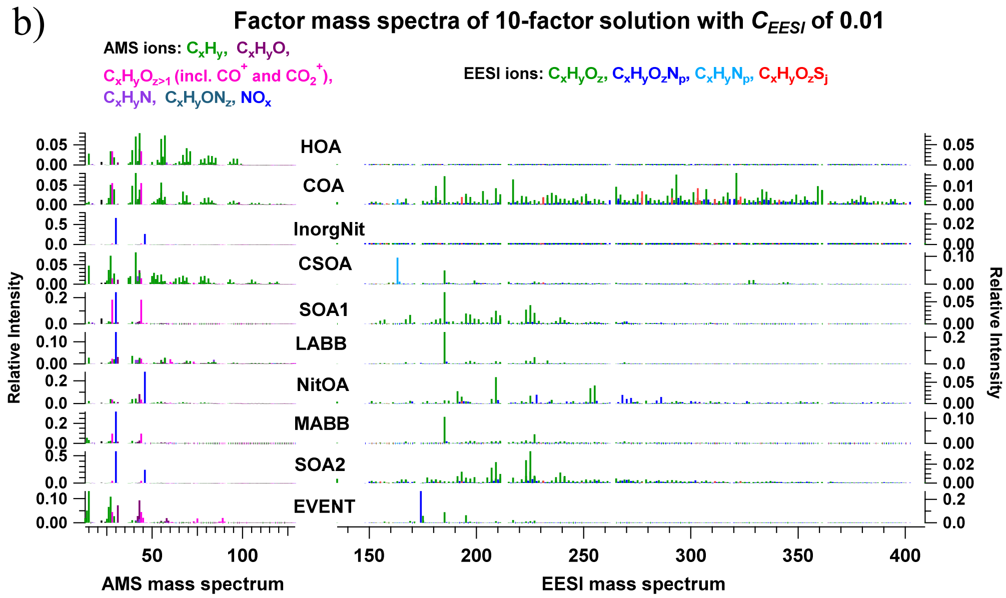

Figure S14. Factor time series in a) and mass spectra in b) for 10-factor solution with C_{EESI} of 0.01 for Zurich winter dataset.

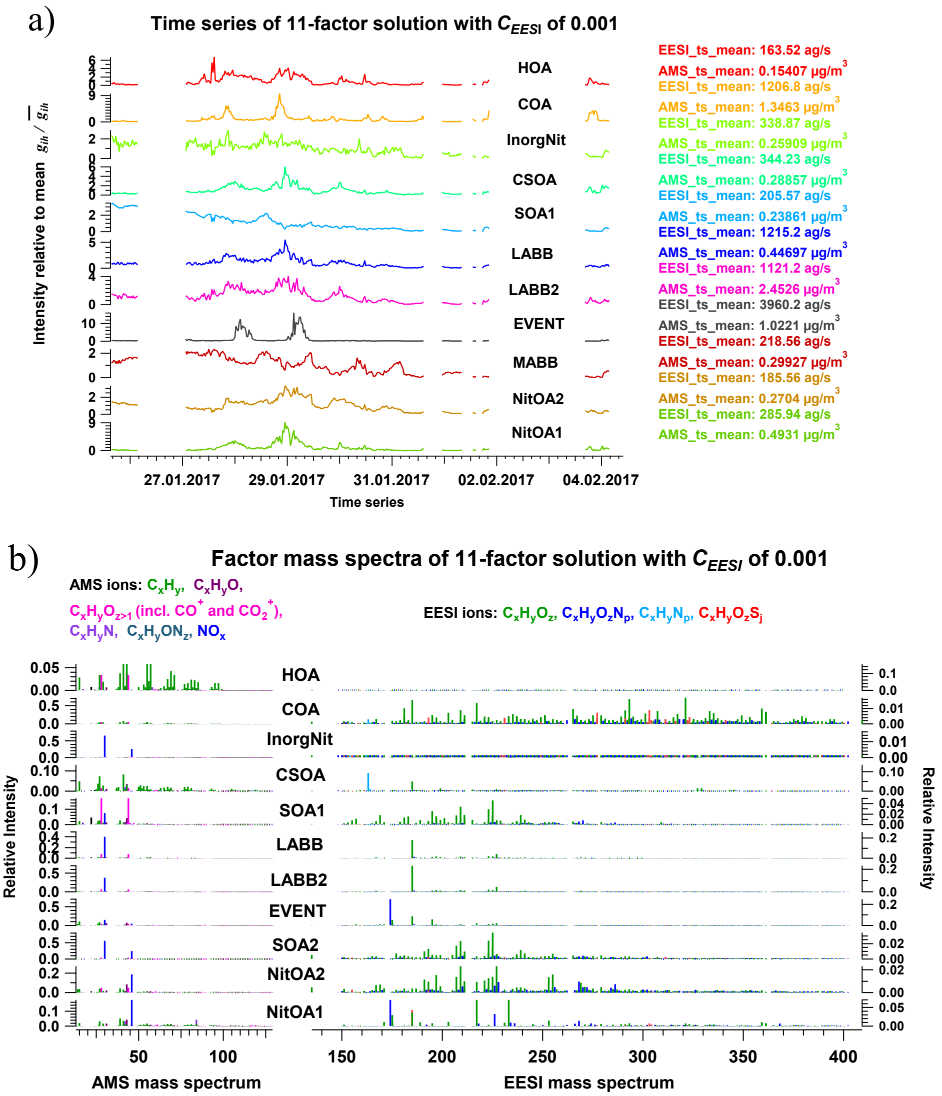

Figure S15. Factor time series in a) and mass spectra in b) for 11-factor solution with C_{EESI} of 0.001 for Zurich winter dataset.

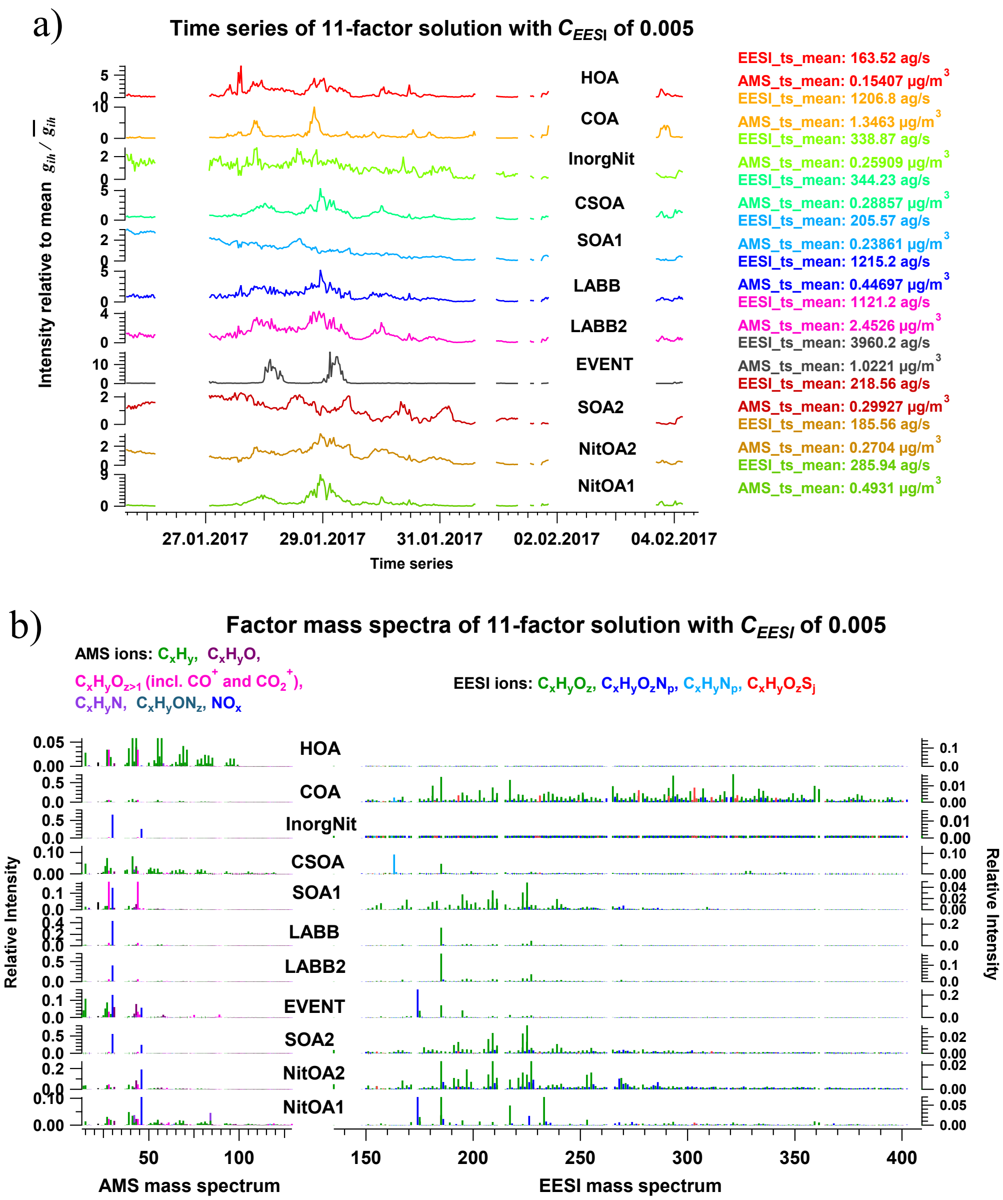

Figure S16. Factor time series in a) and mass spectra in b) for 11-factor solution with C_{EESI} of 0.005 for Zurich winter dataset.

a)

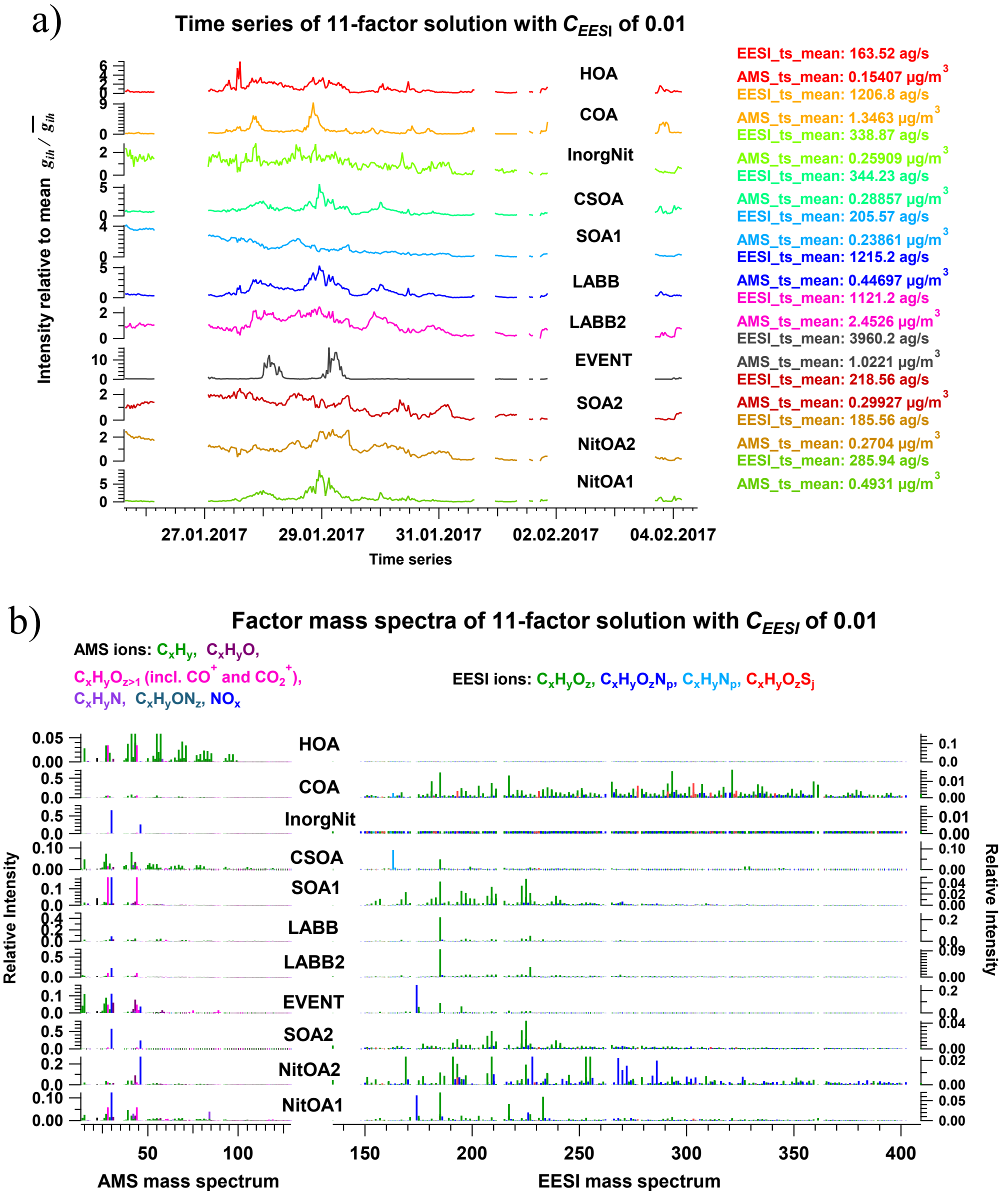

b)

Figure S17. Factor time series in a) and mass spectra in b) for 11-factor solution with C_{EESI} of 0.01 for Zurich winter dataset.

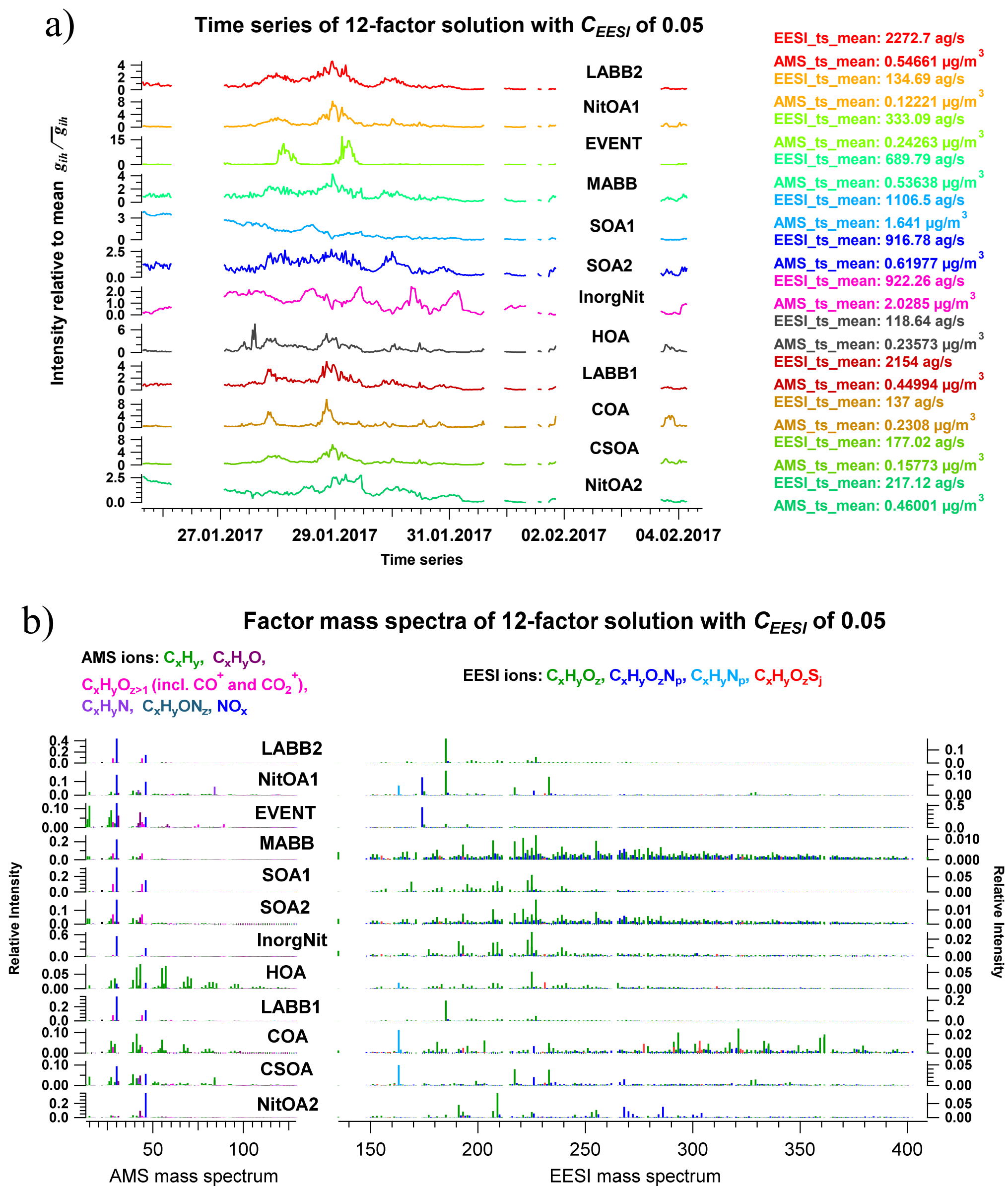

Figure S18. Factor time series in a) and mass spectra in b) for 12-factor solution with C_{EESI} of 0.05 for Zurich winter dataset.

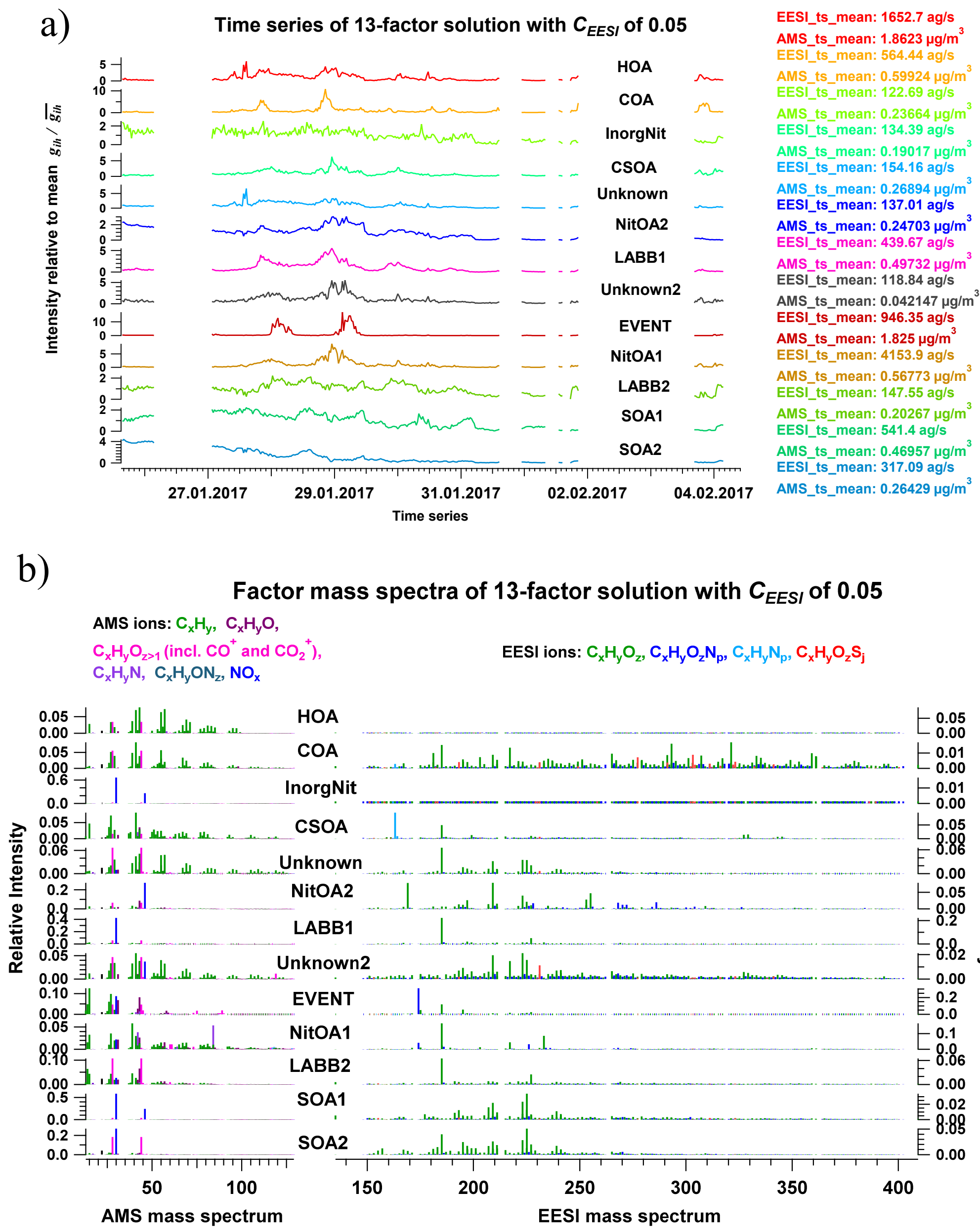

Figure S19. Factor time series in a) and mass spectra in b) for 13-factor solution with C_{EESI} of 0.05 for Zurich winter dataset.

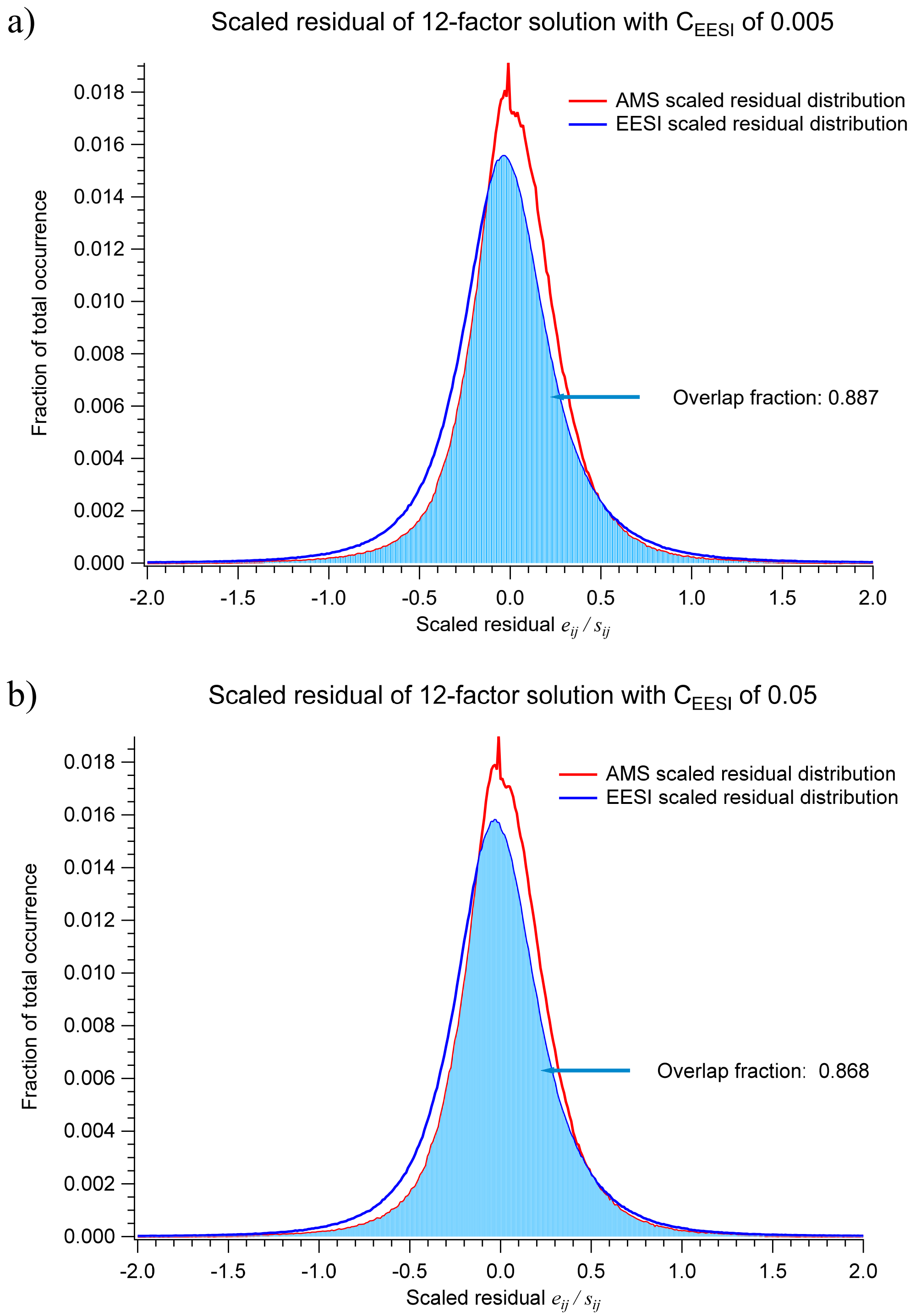

a)
Scaled residual of 12-factor solution with C$_{EESI}$ of 0.005
AMS scaled residual distribution
EESI scaled residual distribution
Overlap fraction: 0.887
Fraction of total occurrence
Scaled residual e_{ij} / s_{ij}
b)
Scaled residual of 12-factor solution with C$_{EESI}$ of 0.05
AMS scaled residual distribution
EESI scaled residual distribution
Overlap fraction: 0.868
Fraction of total occurrence
Scaled residual e_{ij} / s_{ij}

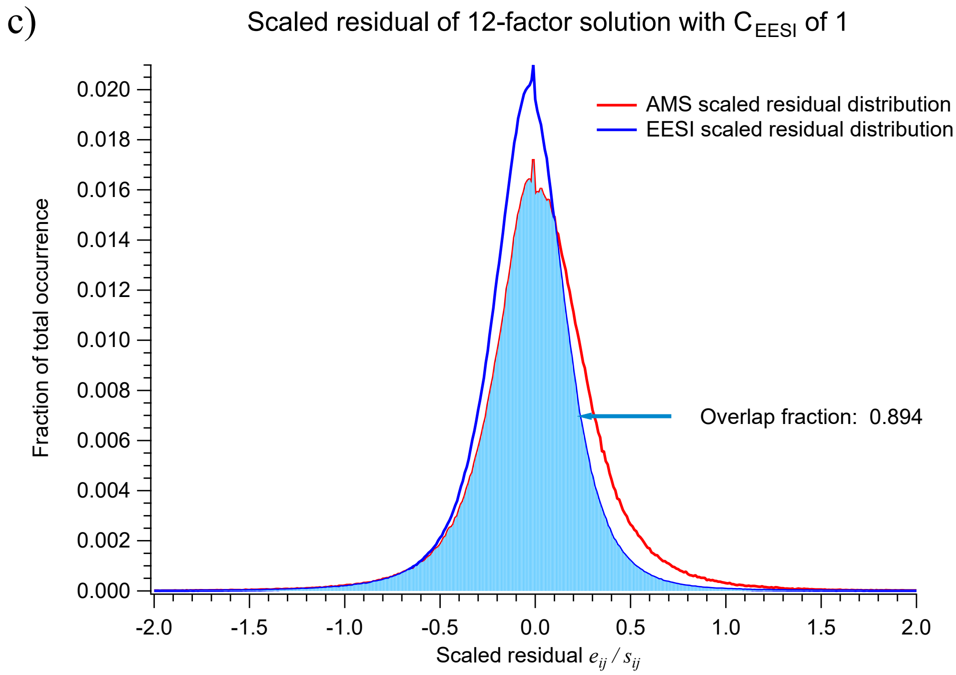

Figure S20. Scaled residual distribution of AMS (red line) and EESI (blue line) in a 12-factor solution from joint dataset in Zurich winter and corresponding overlap fractions when C_{EESI} is equal to 0.005 in a), 0.005 in b), and 1 in c), respectively. Balanced solution is shown in b), whereas in a) and c), AMS and EESI is overweighted, respectively.

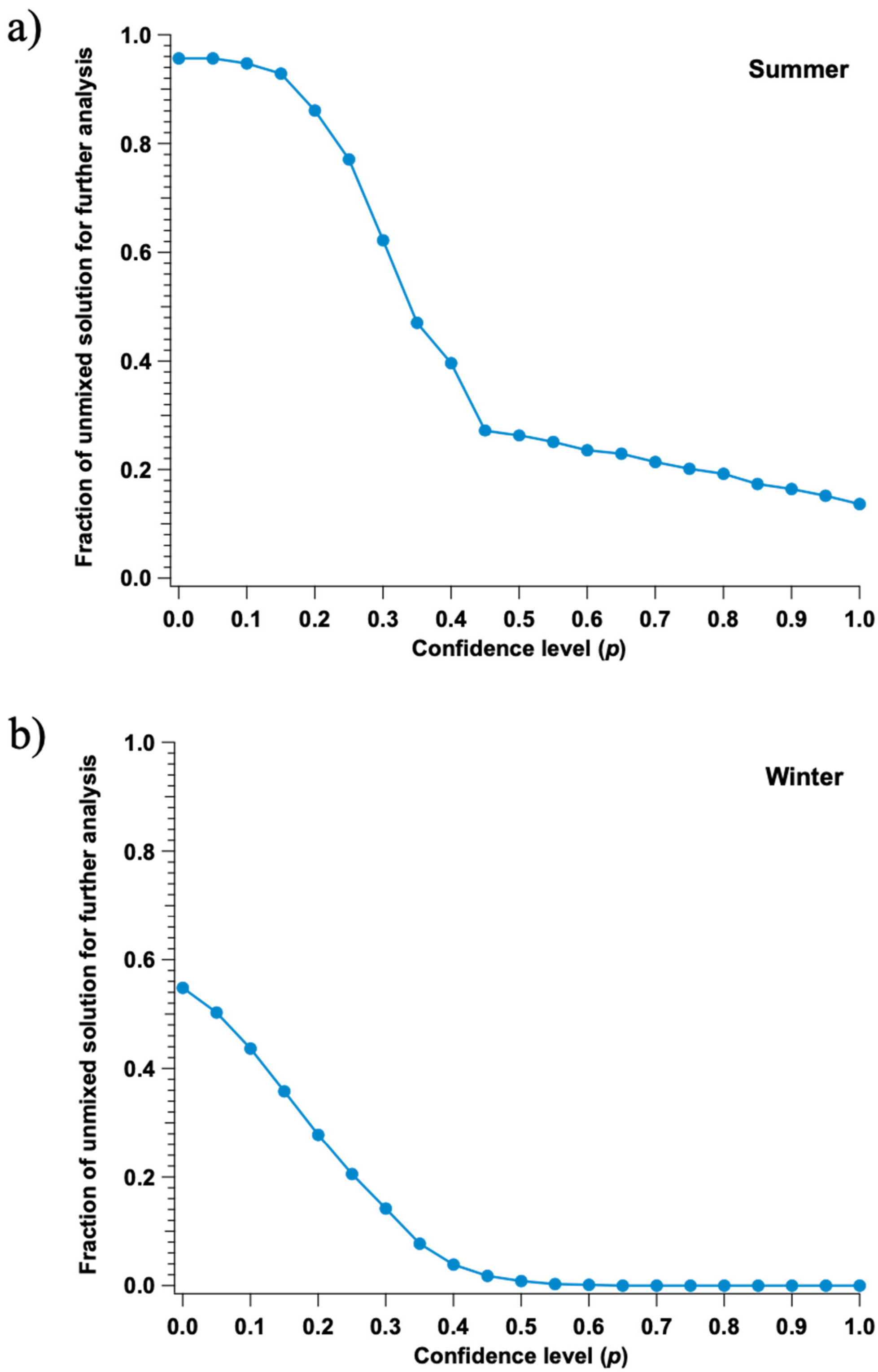

Figure S21. Fraction of unmixed solution selected for further analysis as a function of confidence level (p) for summer dataset in a) and winter dataset in b).

a)

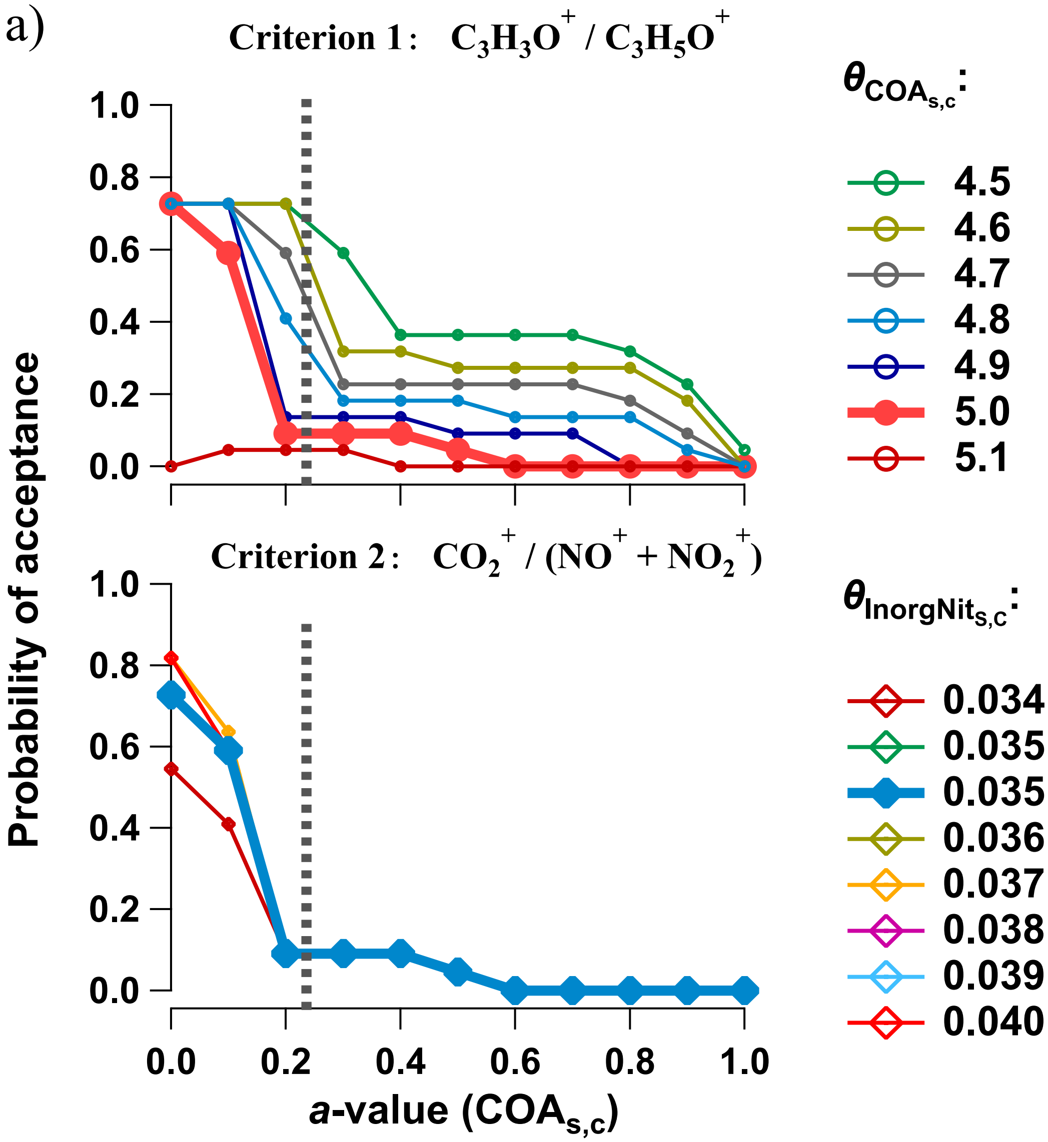

Criterion 1: $C_3H_3O^+ / C_3H_5O^+$
Criterion 2: $CO_2^+ / (NO^+ + NO_2^+)$
Probability of acceptance
1.0
0.8
0.6
0.4
0.2
0.0
a-value ($COA_{s,c}$)
$\theta_{COA_{s,c}}$:
4.5
4.6
4.7
4.8
4.9
5.0
5.1
$\theta_{InorgNit_{s,c}}$:
0.034
0.035
0.035
0.036
0.037
0.038
0.039
0.040

b)

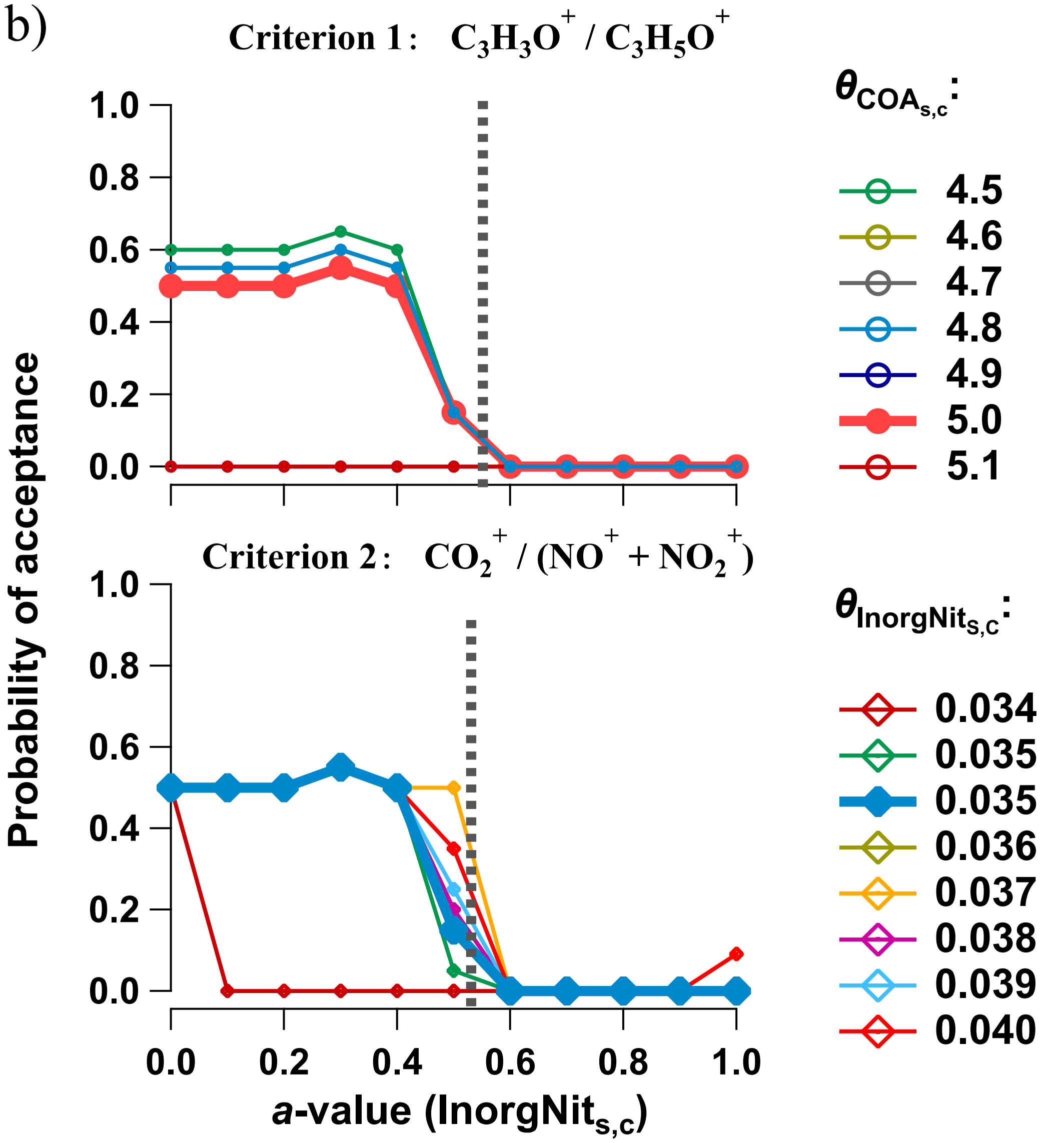

Criterion 1: $C_3H_3O^+ / C_3H_5O^+$
Criterion 2: $CO_2^+ / (NO^+ + NO_2^+)$
Probability of acceptance
a-value ($InorgNit_{s,c}$)
1.0
0.8
0.6
0.4
0.2
0.0
0.0
0.2
0.4
0.6
0.8
1.0
$\theta_{COA_{s,c}}$:
4.5
4.6
4.7
4.8
4.9
5.0
5.1
$\theta_{InorgNit_{s,c}}$:
0.034
0.035
0.035
0.036
0.037
0.038
0.039
0.040

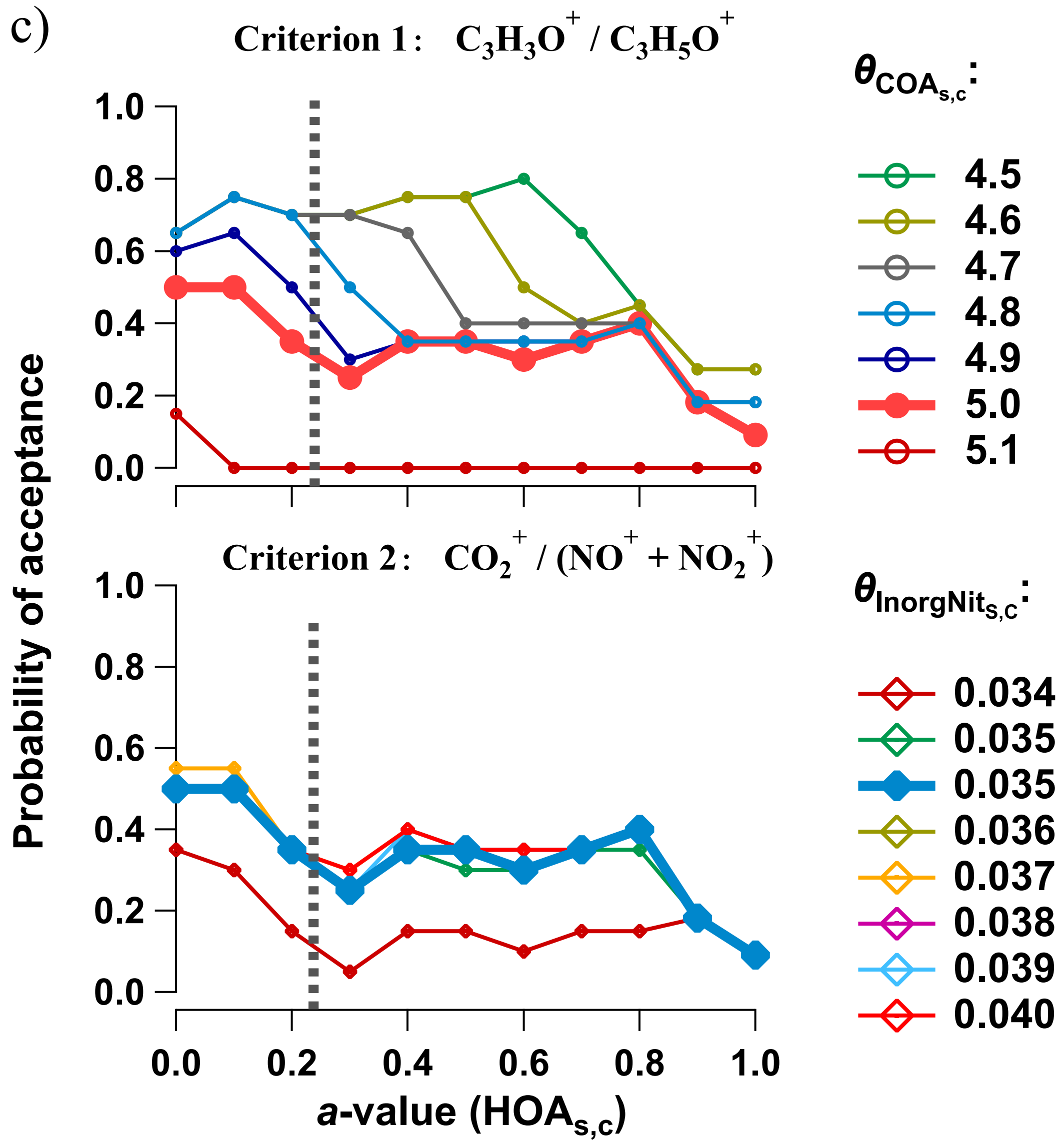

Figure S22. Acceptance probability (i.e., all criteria satisfied simultaneously) calculated from all runs in multi-2D scans as a function of *a*-value of a) $COA_{S,C}$, b) $InorgNit_{S,C}$ and c) $HOA_{S,C}$. To maintain consistency with *a*=0.1 to *a*=1.0, the *a*=0 point considers only runs in which the factor in question is being scanned against a single other factor, discarding runs for which the factor in question is fixed at *a*=0 while two other factors are scanned. Within each sub-figure, the response to different criteria thresholds are shown. Final selected values for criteria thresholds are displayed as a thicker line, while vertical dashed lines denote the final selected upper limit for *a*-value randomisation in the subsequent bootstrap analysis. Note that due to the requirement that all criteria be satisfied simultaneously, the thicker lines (and only the thicker lines) are identical across all panels in a sub-figure. Acceptance requires that a run fulfil all criteria simultaneously.

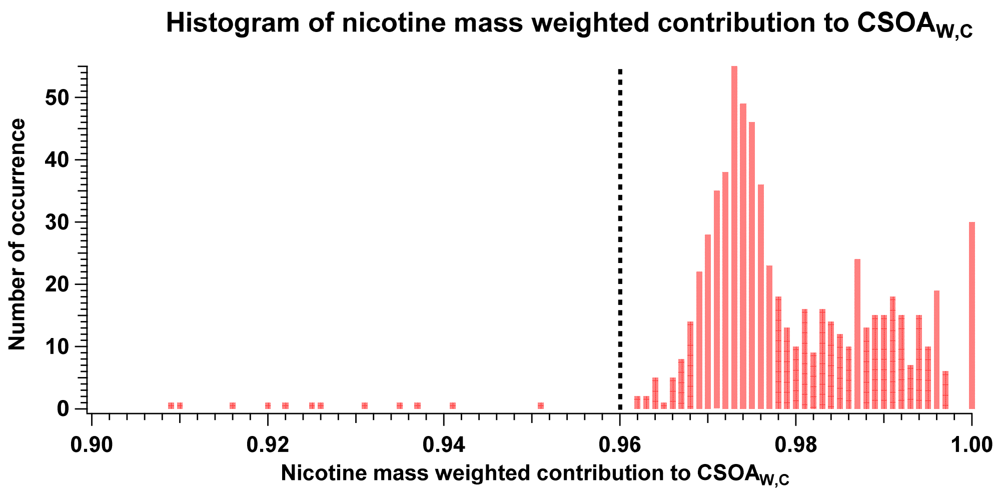

Figure S23. Criteria to select *a*-value range for CSOA$_{W,C}$ factor in Zurich winter dataset. Distribution of mass weighted fraction of nicotine in CSOA$_{W,C}$ for 726 runs, with 396 runs with *a*-value of 0 and 33 runs for each a-value from 0.1 to 1. The mass weighted fraction of nicotine apportioned to CSOA$_{W,C}$ in most runs are higher in 0.96.

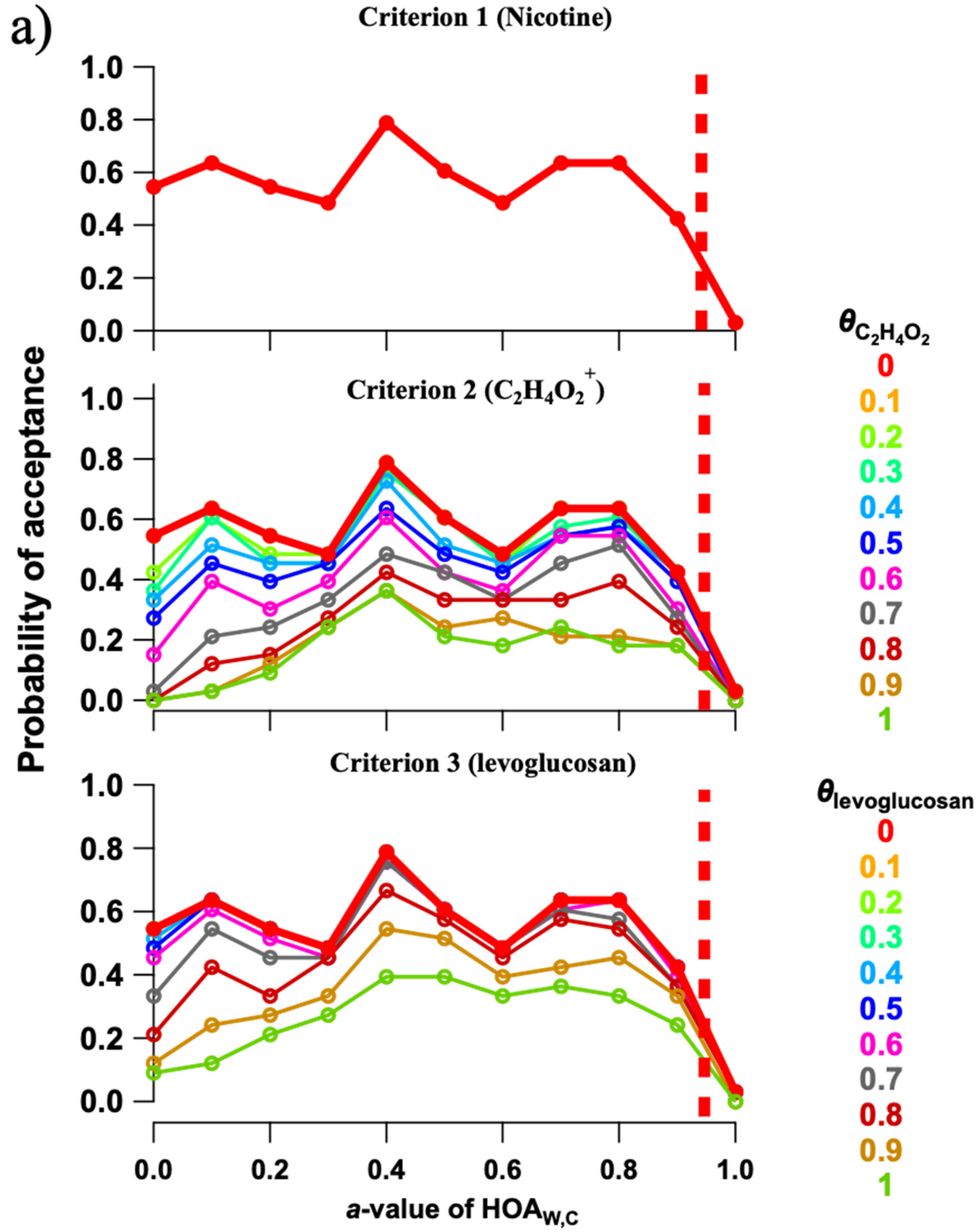
a)
Criterion 1 (Nicotine)
Criterion 2 ($C_2H_4O_2^+$)
Criterion 3 (levoglucosan)
Probability of acceptance
a-value of $HOA_{W,C}$
$\theta_{C_2H_4O_2}$
0
0.1
0.2
0.3
0.4
0.5
0.6
0.7
0.8
0.9
1
$\theta_{levoglucosan}$
0
0.1
0.2
0.3
0.4
0.5
0.6
0.7
0.8
0.9
1

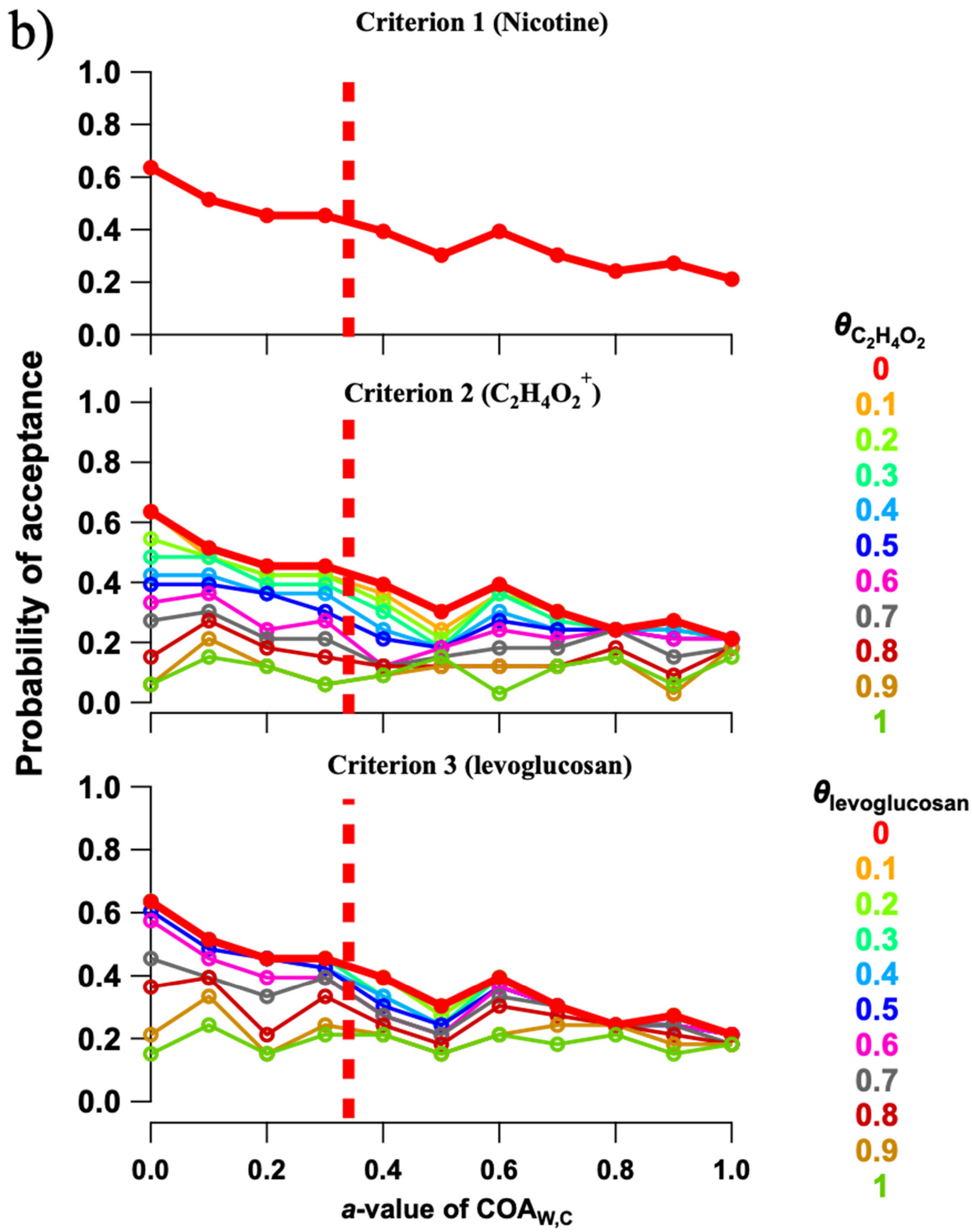

b)
Criterion 1 (Nicotine)
Criterion 2 ($C_2H_4O_2^+$)
Criterion 3 (levoglucosan)
Probability of acceptance
1.0
0.8
0.6
0.4
0.2
0.0
0.0
0.2
0.4
0.6
0.8
1.0
a-value of $COA_{W,C}$
$\theta_{C_2H_4O_2}$
$\theta_{levoglucosan}$
0
0.1
0.2
0.3
0.4
0.5
0.6
0.7
0.8
0.9
1

c)

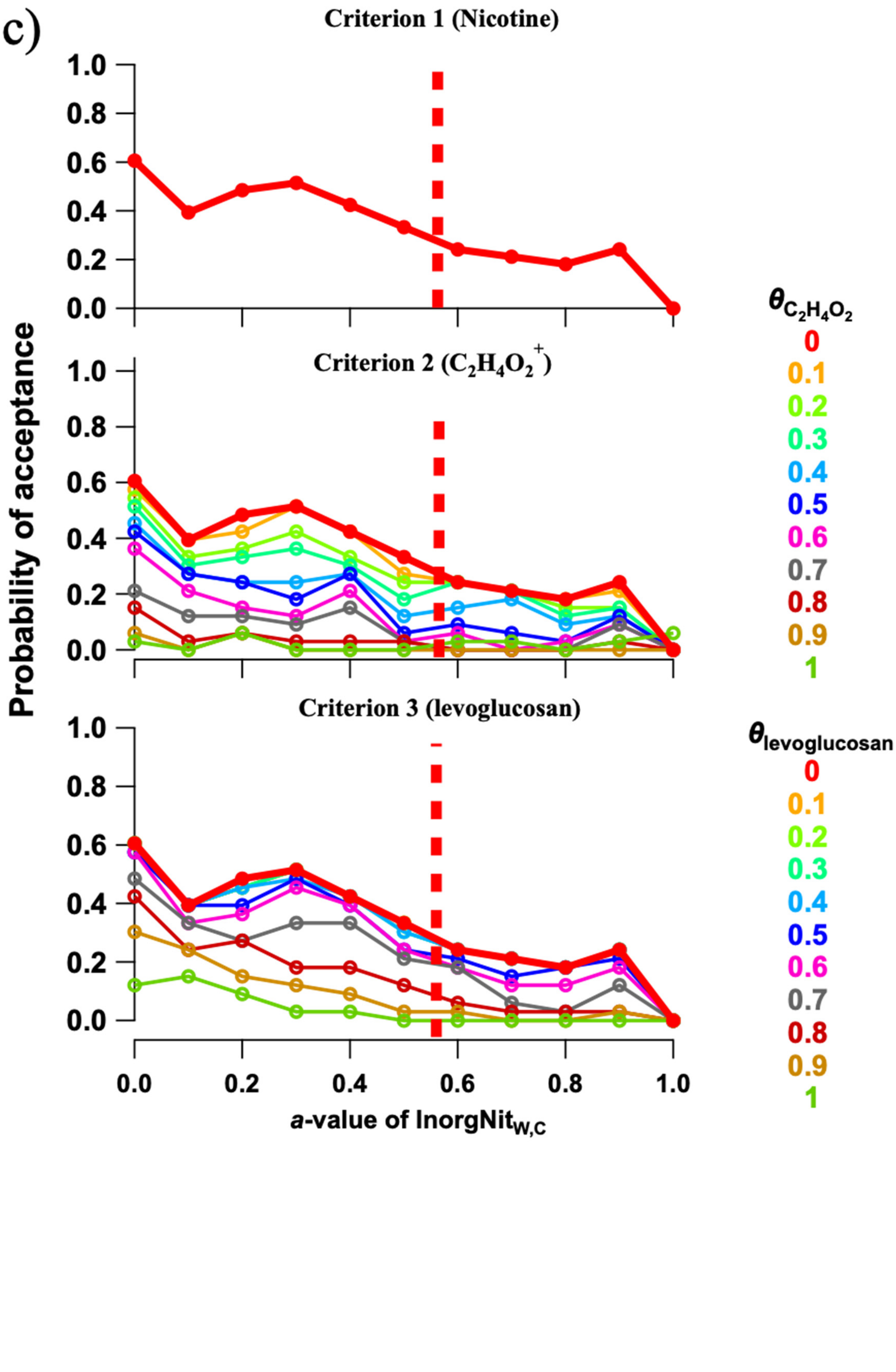

Criterion 1 (Nicotine)
Criterion 2 ($C_2H_4O_2^+$)
Criterion 3 (levoglucosan)
Probability of acceptance
$\theta_{C_2H_4O_2}$
$\theta_{levoglucosan}$
0
0.1
0.2
0.3
0.4
0.5
0.6
0.7
0.8
0.9
1
a-value of $InorgNit_{W,C}$

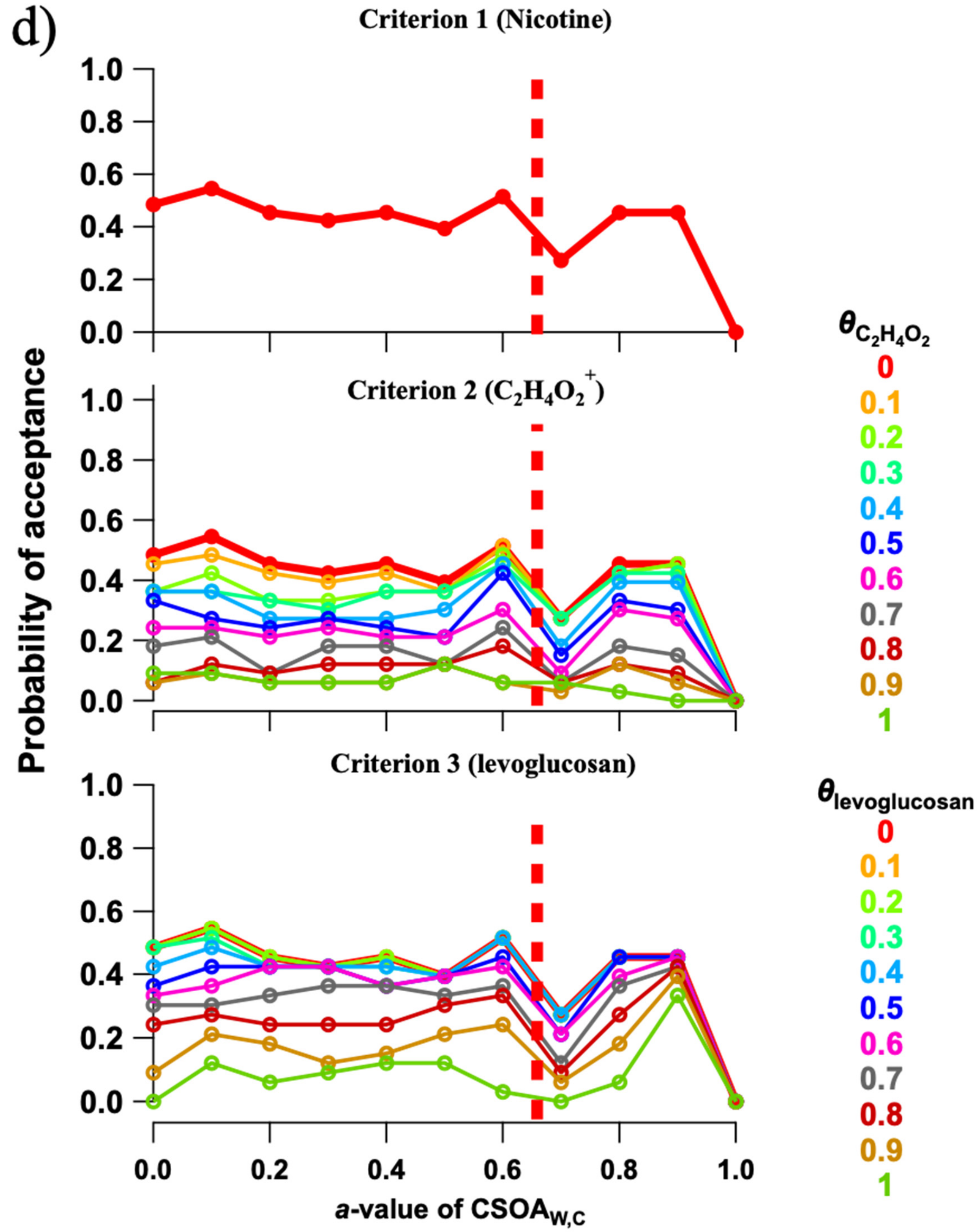

Figure S24. Acceptance probability (i.e., all criteria satisfied simultaneously) calculated from all runs in multi-2D scans as a function of a-value of a) $HOA_{W,C}$, b) $COA_{W,C}$, c) $InorgNit_{W,C}$ and d) $CSOA_{w,C}$. To maintain consistency with a=0.1 to a=1.0, the a=0 point considers only runs in which the factor in question is being scanned against a single other factor, discarding runs for which the factor in question is fixed at a=0 while two other factors are scanned. Within each sub-figure, the response to different criteria thresholds are shown. Final selected values for criteria thresholds are displayed as a thicker line, while vertical dashed lines denote the final selected upper limit for a-value randomisation in the subsequent bootstrap analysis. Note that due to the requirement that all criteria be satisfied simultaneously, the thicker lines (and only the thicker lines) are identical across all panels in a sub-figure. Acceptance requires that a run fulfil all criteria simultaneously.

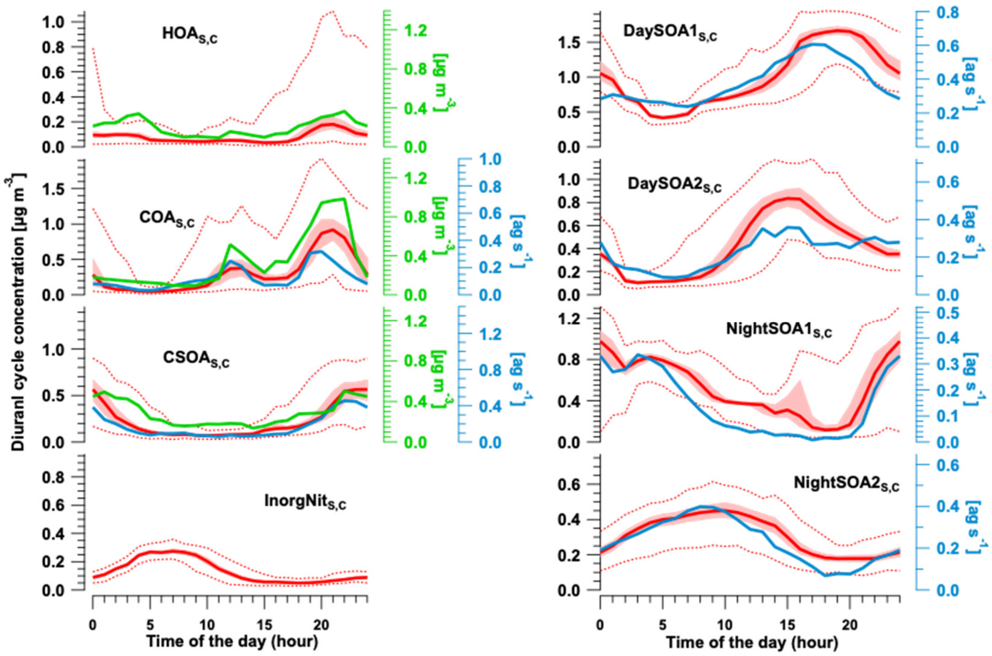

Figure S25. Diurnal cycle of median accepted 764 runs in Zurich Summer dataset, represented in red lines, shaded area indicates the interquartile range, dashed lines are the maximum and minimum value of diurnal cycle calculation.

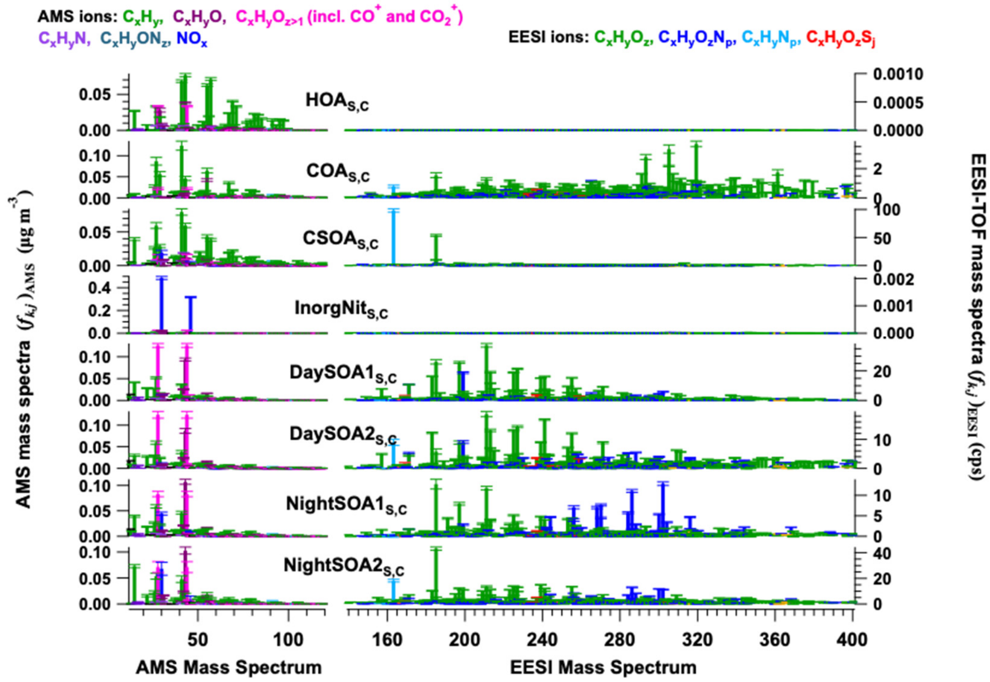

Figure S26. Average factor profiles of 764 accepted bootstrap runs in Zurich Summer dataset, coloured by different ion families, with error bars of mean±standard deviation. Note, both AMS and EESI-TOF factor profiles are normalised, according to Eq. 9.

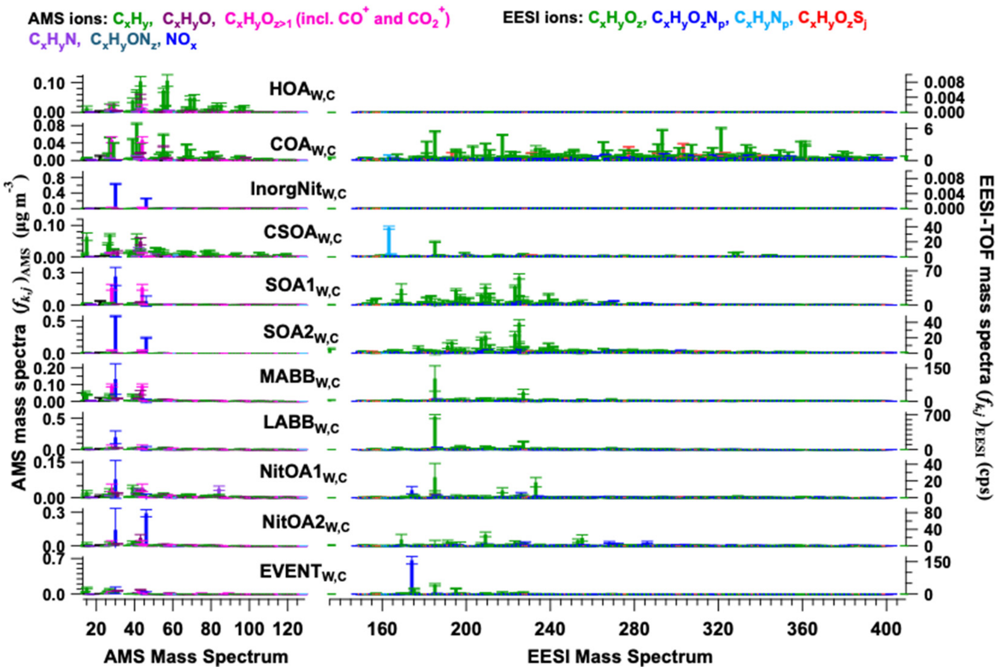

Figure S27. Average factor profiles of 308 accepted bootstrap runs in Zurich winter dataset, coloured by different ion families, with error bars of mean±standard deviation. Note, both AMS and EESI-TOF factor profiles are normalised, according to Eq. 9.

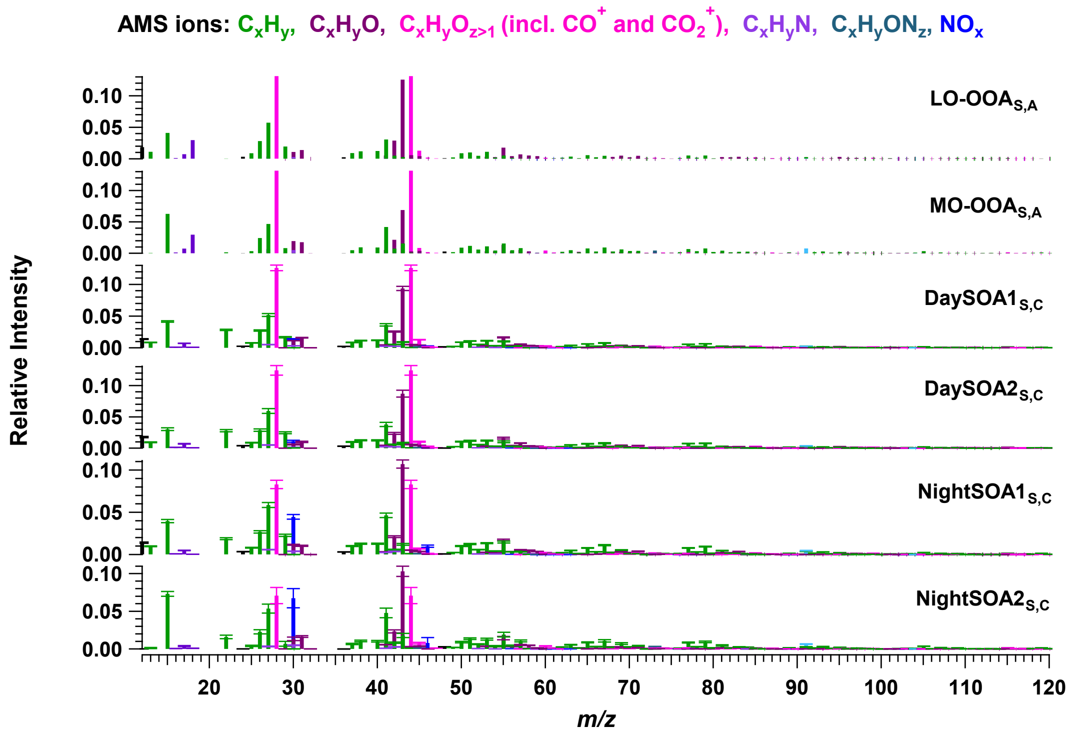

Figure S28. Factor profiles of LO-OOA$_{S,A}$ and MO-OOA$_{S,A}$ from AMS-only PMF analysis and four SOAs (DaySOA1$_{S,A}$, DaySOA2$_{S,A}$, NightSOA1$_{S,A}$ and NightSOA2$_{S,A}$) resolved from combined PMF analysis for summer.

a)

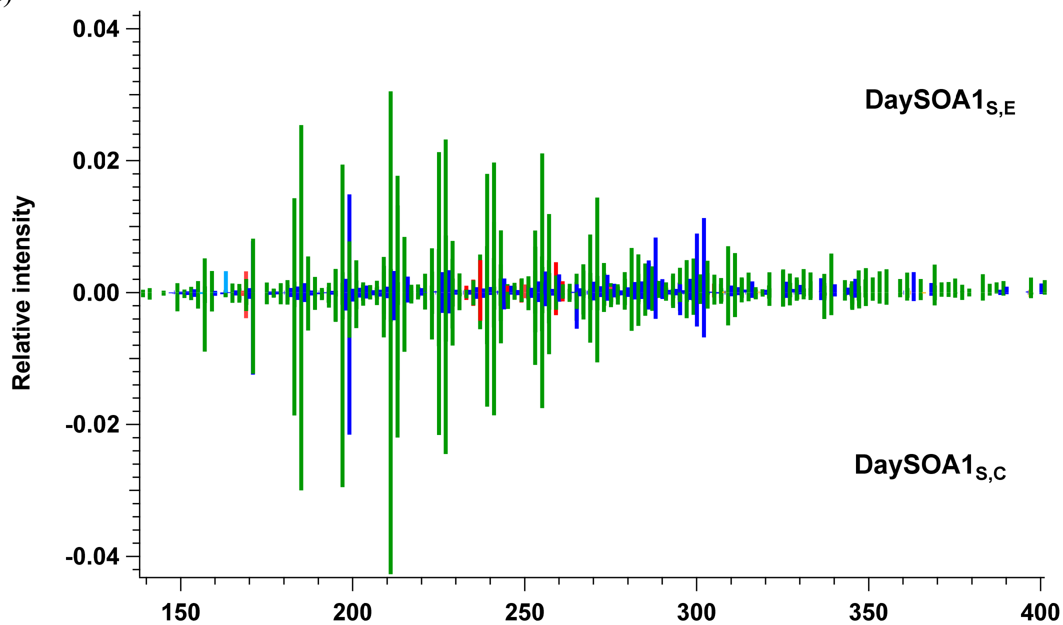
0.04
0.02
0.00
-0.02
-0.04
Relative intensity
DaySOA1$_{S,E}$
DaySOA1$_{S,C}$
150
200
250
300
350
400

b)

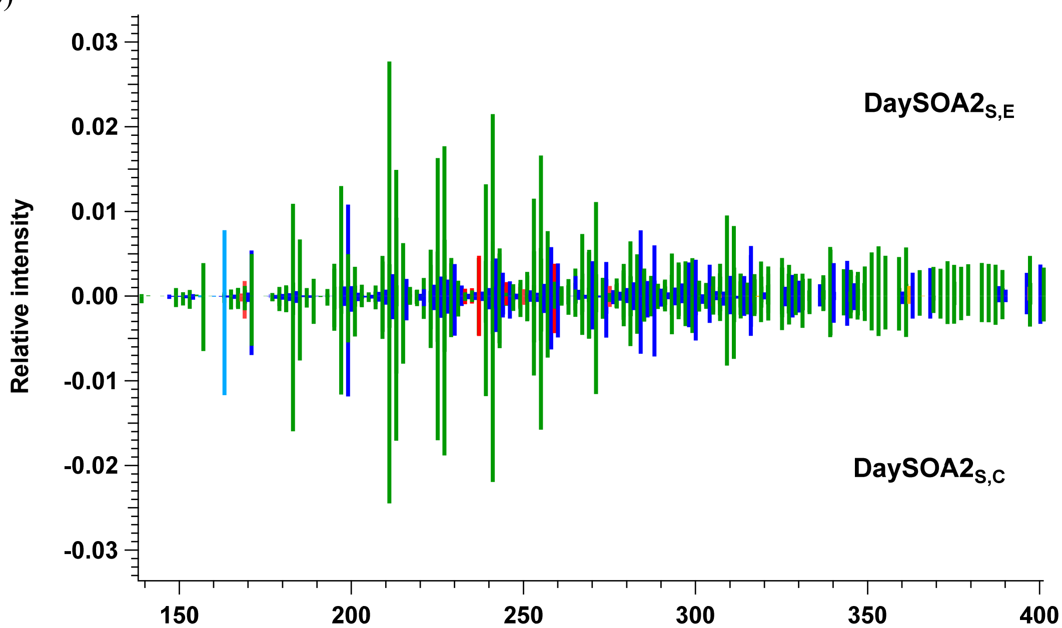
0.03
0.02
0.01
0.00
-0.01
-0.02
-0.03
Relative intensity
DaySOA2$_{S,E}$
DaySOA2$_{S,C}$
150
200
250
300
350
400

c)

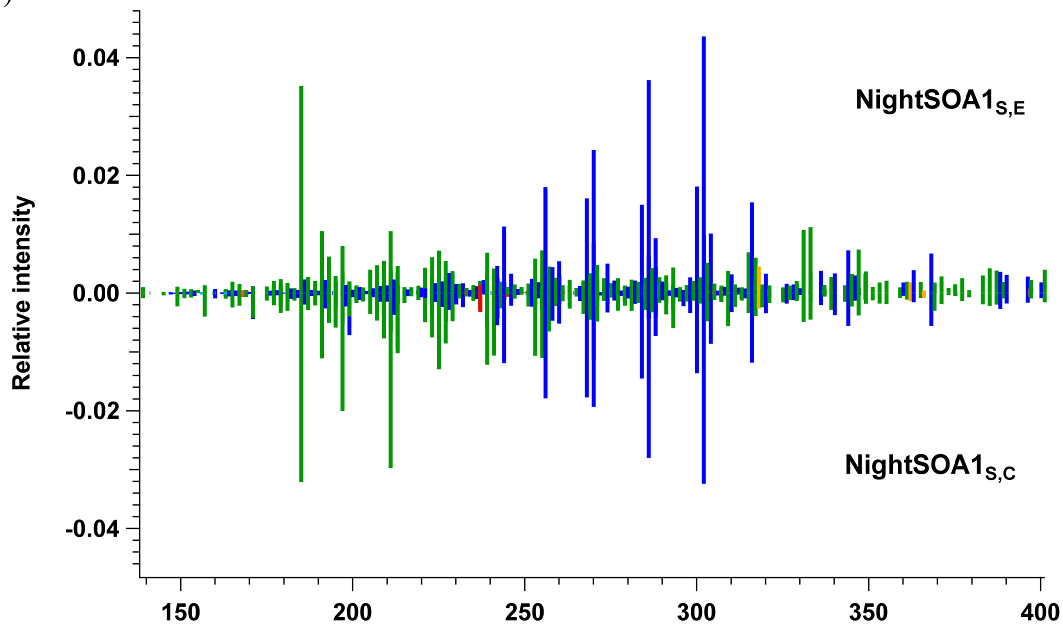

d)

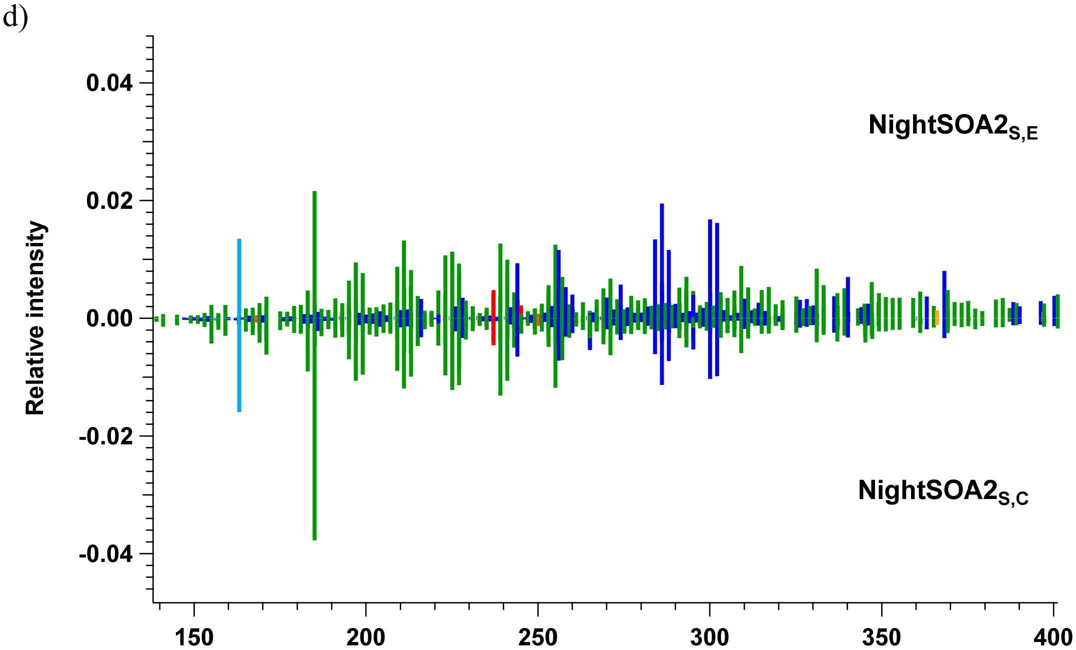

Figure S29. Comparison of four summer SOA factors (DaySOA1$_{S,E}$, DaySOA2$_{S,E}$, NightSOA1$_{S,E}$ and NightSOA2$_{S,E}$) resolved from EESI-TOF-only PMF analysis to the corresponding factors (DaySOA1$_{S,C}$, DaySOA2$_{S,C}$, NightSOA1$_{S,C}$ and NightSOA2$_{S,C}$) resolved from the combined PMF analysis.

a)

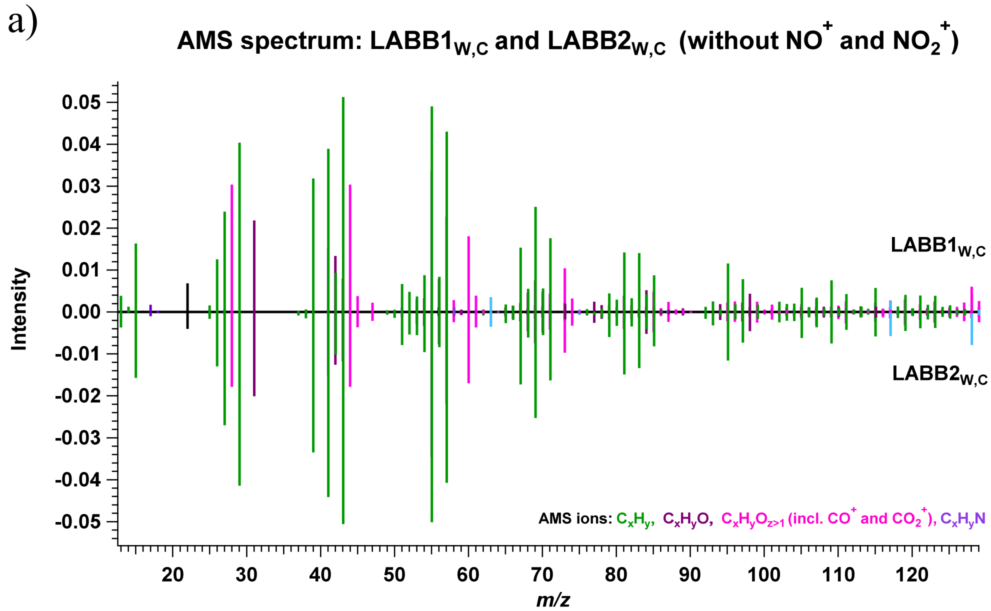

b)

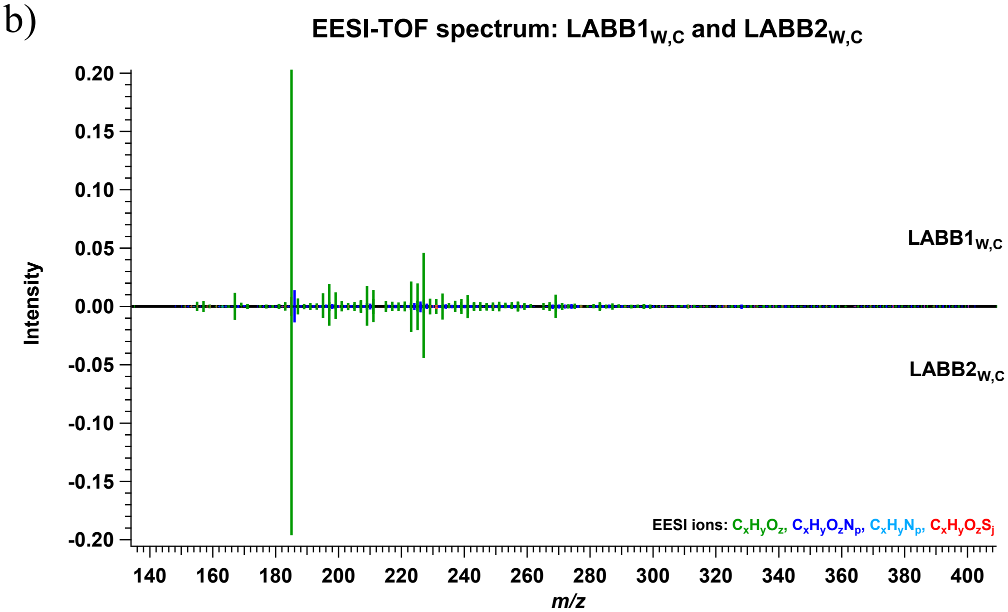

Figure S30. Comparison of two $LABB_{W,C}$ factors resolved from combined dataset in Zurich winter. AMS part mass spectra comparison without NO^+ and NO_2^+ is shown in a), and EESI-TOF part mass spectra comparison is shown in b). Both figures are coloured by different ion groups.

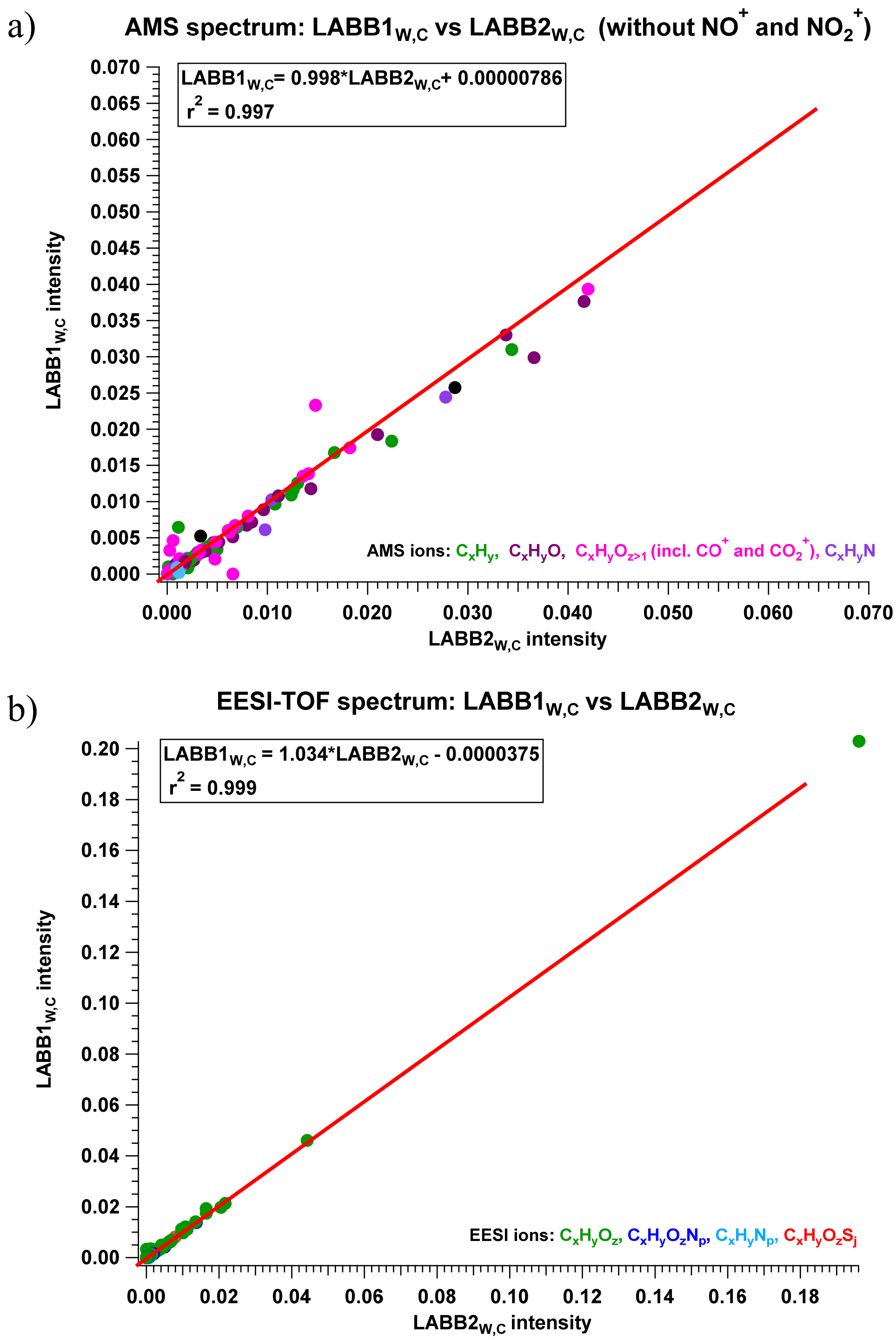

Figure S31. Comparison of two $LABB_{W,C}$ factors resolved from the combined dataset in Zurich winter. Scatter plot of AMS ions without NO^+ and NO_2^+ is shown in a), and scatter plot of EESI ions is shown in b). In both figures, correlation of ion intensity of $LABB1_{W,C}$ and $LABB2_{W,C}$ is higher than 0.99 with slope around 1.

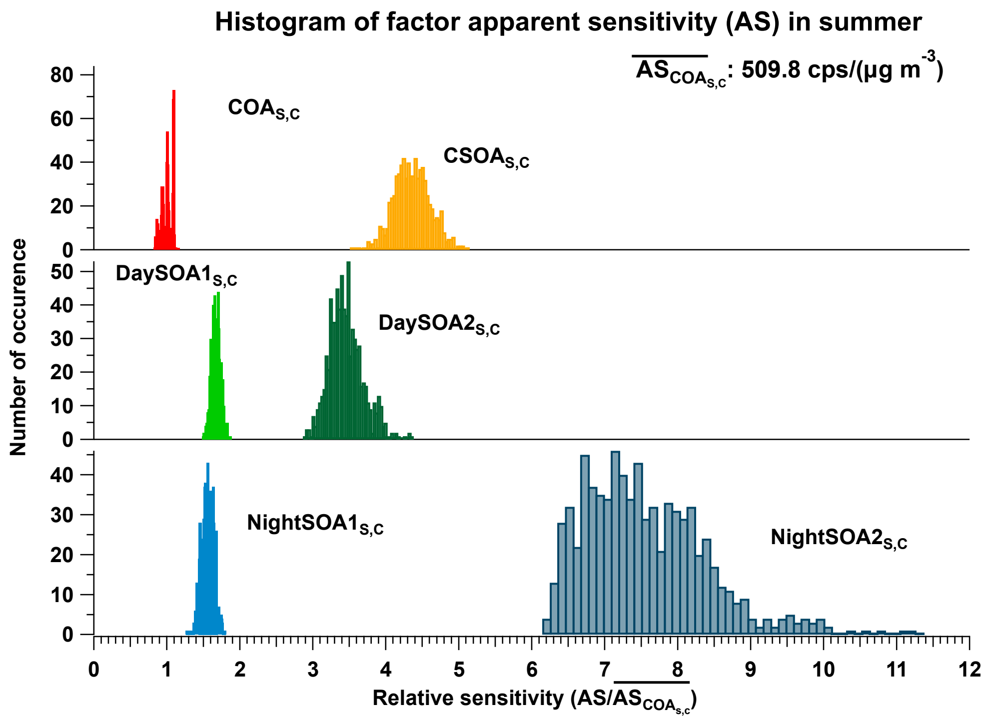

Figure S32. Histogram of factor EESI-TOF relative sensitivity to two primary sources and four secondary sources normalised by EESI-TOF sensitivity to $COA_{S,C}$ in Zurich summer campaign. Relative sensitivity is calculated as apparent sensitivity (AS_k) to a factor over mean apparent sensitivity to COA.

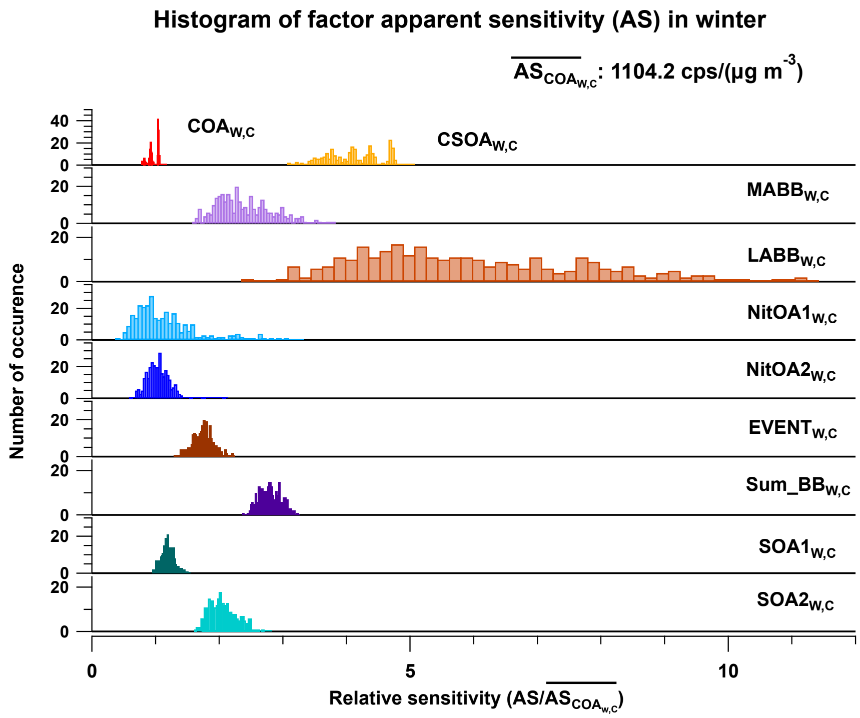

Figure S33. Histogram of factor relative sensitivity to two primary sources, two aged-biomass burning factors, two nitrogen-related sources, one event-specific factor, two secondary sources, and the sum of biomass burning related factors. Relative sensitivity is calculated as the apparent sensitivity (AS_k) to a factor over the mean apparent sensitivity to $COA_{W,C}$.

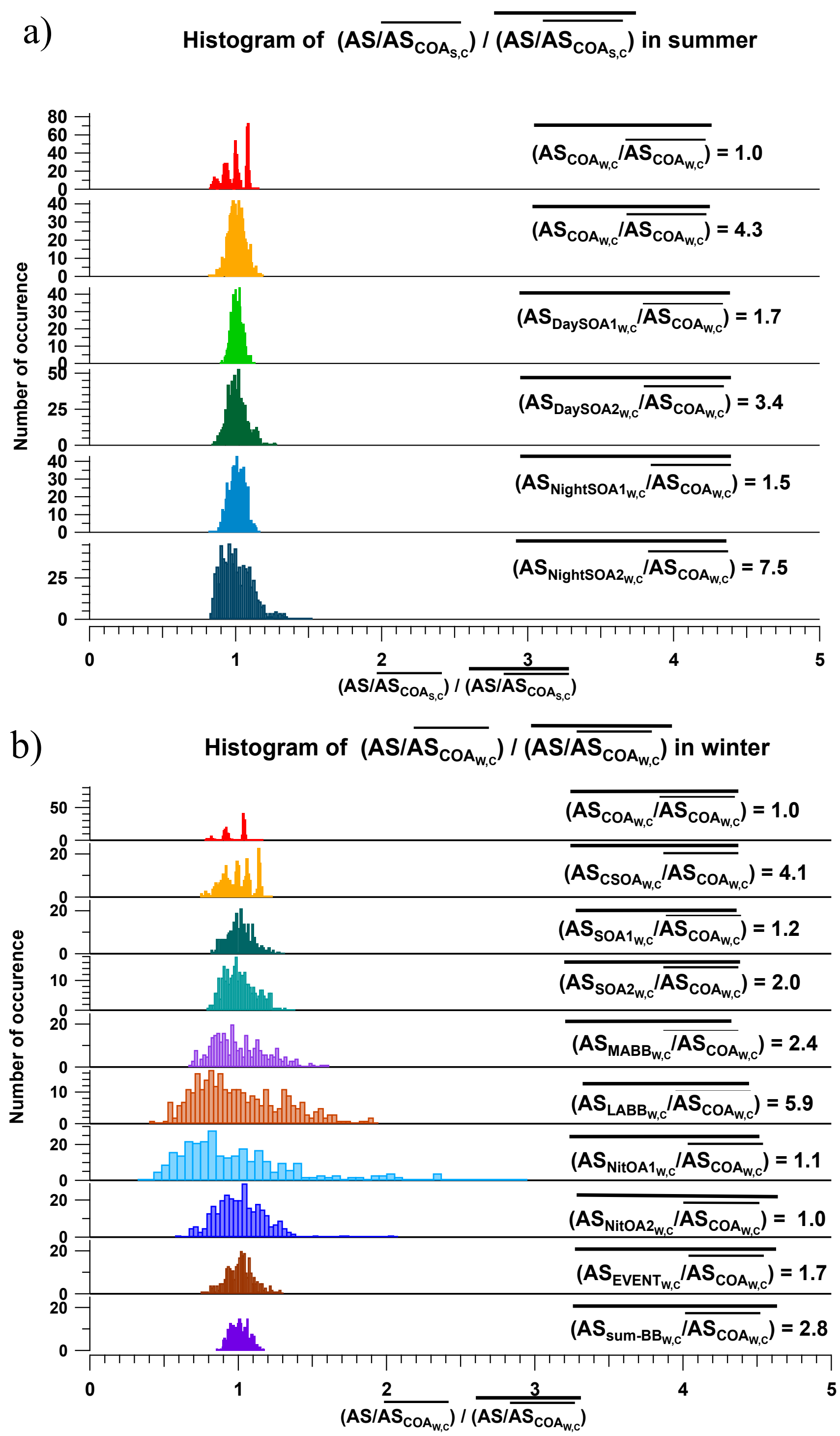

Figure S34. Histogram of ratio of the relative apparent sensitivity $AS/\overline{AS_{\mathrm{COA}}}$ to the mean relative apparent sensitivity $\overline{AS/\overline{AS_{\mathrm{COA}}}}$ for primary sources and secondary sources a) within 764 accepted runs in Zurich summer campaign and b) within 308 accepted runs in Zurich winter campaign. Note in b) the sum of biomass burning related factors (denoted Sum-$BB_{W,C}$) is calculated from $MABB_{W,C}$, $LABB_{W,C}$, $NitOA2_{W,C}$, $NitOA2_{W,C}$ and $EVENT_{W,C}$. In this plot, all the distributions are re-centred to 1, and the width of the distribution represents the relative uncertainty of the corresponding factor.

Table S1. Summary of relevant quantities to estimate $frac_{\mathrm{ON},k}$ and corresponding $\sum_j (f_{k,j})_{\mathrm{AMS},k}$, with different R_{ON} for each unconstrained factor from combined PMF analysis for summer and winter. Note that the HOA, COA, and CSOA in both factors are constrained to have zero contribution from NO^+ and NO_2^+.

Summer								
NH_4NO_3 reference: $f_{\mathrm{NO^+}}$ = 0.487, $f_{\mathrm{NO_2^+}}$ = 0.318, R_{cal} = 0.688								
			R_{ON} = 0.08		R_{ON} = 0.14		R_{ON} = 0.20	
Factor	$f_{\mathrm{NO^+}}$	$f_{\mathrm{NO_2^+}}$	$frac_{\mathrm{ON}}$	$\frac{\sum_j (f_{k,j})_{\mathrm{AMS,OA}}}{\sum_j (f_{k,j})_{\mathrm{AMS,all}}}$	$frac_{\mathrm{ON}}$	$\frac{\sum_j (f_{k,j})_{\mathrm{AMS,OA}}}{\sum_j (f_{k,j})_{\mathrm{AMS,all}}}$	$frac_{\mathrm{ON}}$	$\frac{\sum_j (f_{k,j})_{\mathrm{AMS,OA}}}{\sum_j (f_{k,j})_{\mathrm{AMS,all}}}$
$HOA_{S,C}$	0	0	0	1	0	1	0	1
$COA_{S,C}$	0	0	0	1	0	1	0	1
$InorgNit_{S,C}$ [1*]	0.486	0.318	0.0358	0.225	0.0420	0.230	0.0496	0.236
$CSOA_{S,C}$	0	0	0	1	0	0.995	0	1
$DaySOA1_{S,C}$	0.0137	0.00262	0.742	0.996	0.869	0.998	1.000	1.000
$DaySOA2_{S,C}$	0.0111	0.00103	0.969	1.000	1.000	1.000	1.000	1.000
$NightSOA1_{S,C}$	0.0445	0.00979	0.682	0.983	0.798	0.989	0.944	0.997
$NightSOA2_{S,C}$	0.0679	0.00824	0.897	0.993	1	1	1	1
Winter								
NH_4NO_3 reference: $f_{\mathrm{NO^+}}$ = 0.630, $f_{\mathrm{NO_2^+}}$ = 0.248, R_{cal} = 0.394								
			R_{ON} = 0.08		R_{ON} = 0.14		R_{ON} = 0.20	
Factor	$f_{\mathrm{NO^+}}$	$f_{\mathrm{NO_2^+}}$	$frac_{\mathrm{ON}}$	$\frac{\sum_j (f_{k,j})_{\mathrm{AMS,OA}}}{\sum_j (f_{k,j})_{\mathrm{AMS,all}}}$	$frac_{\mathrm{ON}}$	$\frac{\sum_j (f_{k,j})_{\mathrm{AMS,OA}}}{\sum_j (f_{k,j})_{\mathrm{AMS,all}}}$	$frac_{\mathrm{ON}}$	$\frac{\sum_j (f_{k,j})_{\mathrm{AMS,OA}}}{\sum_j (f_{k,j})_{\mathrm{AMS,all}}}$
$HOA_{W,C}$	0	0	0	1	0	1	0	1
$COA_{W,C}$	0	0	0	1	0	1	0	1
$InorgNit_{W,C}$ [1*]	0.636	0.263	0	0.101	0	0.101	0	0.101
$CSOA_{W,C}$	0	0	0	1	0	1	0	1
$SOA1_{W,C}$	0.264	0.0347	0.799	0.940	1	1	1	1
$SOA2_{W,C}$	0.570	0.238	0 [2*]	0.192	0 [2*]	0.192	0 [2*]	0.192
$MABB_{W,C}$	0.133	0.00185	1	1	1	1	1	1
$LABB_{W,C}$	0.195	0.0176	0.958	0.991	1	1	1	1
$NitOA1_{W,C}$	0.0781	0.00260	1	1	1	1	1	1
$NitOA2_{W,C}$	0.143	0.293	0 [2*]	0.564	0 [2*]	0.564	0 [2*]	0.564
$EVENT_{W,C}$	0.0736	0.0203	0.319	0.936	0.416	0.945	0.572	0.960

Note 1*: The $frac_{\mathrm{ON}}$ for InorgNit is not 0 due to the uncertainties in the constraint. $\frac{\sum_j (f_{k,j})_{\mathrm{AMS,OA}}}{\sum_j (f_{k,j})_{\mathrm{AMS,all}}}$ in this factor is not 0 due to the uncertainties in the constraint and the CO_2^+ resulted from NH_4NO_3 which is also included in the reference profiles (Pieber et al., 2016).

Note 2*: according to Eq. 18, the $frac_{\mathrm{ON}}$ is negative, therefore, we regarded all signals from NO^+ and NO_2^+ as inorganics, and set $frac_{\mathrm{ON}}$ to be 0.

Table S2. Summary of the median value of the ratio of standard deviation to mean factor concentration over accepted runs at each time point for summer and winter factors.

Factor	(Standard deviation / mean factor concentration)$_{median}$
$HOA_{S,C}$	7.4%
$COA_{S,C}$	4.5%
$InorgNit_{S,C}$	5.2%
$CSOA_{S,C}$	3.2%
$DaySOA1_{S,C}$	5.4%
$DaySOA2_{S,C}$	1.4%
$NightSOA1_{S,C}$	0.6%
$NightSOA2_{S,C}$	4.3%
$HOA_{W,C}$	12.8%
$COA_{W,C}$	14.5%
$InorgNit_{W,C}$	26.5%
$CSOA_{W,C}$	13.7%
$SOA1_{W,C}$	12.2%
$SOA2_{W,C}$	18.5%
$MABB_{W,C}$	24.1%
$LABB_{W,C}$	18.1%
$NitOA1_{W,C}$	24.3%
$NitOA2_{W,C}$	35.1%
$EVENT_{W,C}$	3.5%

Table S3. Summary of apparent sensitivities for factors retrieved from combined PMF analysis for summer and winter.

Factor	Factor apparent sensitivity (AS_k) (cps /(μg m^{-3}))
$COA_{S,C}$	5.09 (± 0.45) × 10^2
$CSOA_{S,C}$	22.10 (± 1.27) × 10^2
$DaySOA1_{S,C}$	8.45 (± 0.32) × 10^2
$DaySOA2_{S,C}$	17.47 (± 1.20) × 10^2
$NightSOA1_{S,C}$	7.86 (± 0.43) × 10^2
$NightSOA2_{S,C}$	38.23 (± 4.33) × 10^2
Bulk $OA_{S,C}$	**12.54 (± 0.10) × 10^2**
$COA_{W,C}$	1.10 (± 0.13) × 10^3
$CSOA_{W,C}$	4.56 (± 0.54) × 10^3
$SOA1_{W,C}$	1.29 (± 0.11) × 10^3
$SOA2_{W,C}$	2.25 (± 0.24) × 10^3
$MABB_{W,C}$	2.62 (± 0.49) × 10^3
$LABB_{W,C}$	6.51 (± 2.01) × 10^3
$NitOA1_{W,C}$	1.43 (± 0.57) × 10^3
$NitOA2_{W,C}$	1.12 (± 0.21) × 10^3
$EVENT_{W,C}$	1.93 (± 0.18) × 10^3
Bulk $OA_{W,C}$	**2.27 (± 0.07) × 10^3**

Reference

Pieber, S. M., El Haddad, I., Slowik, J. G., Canagaratna, M. R., Jayne, J. T., Platt, S. M., Bozzetti, C., Daellenbach, K. R., Frohlich, R., Vlachou, A., Klein, F., Dommen, J., Miljevic, B., Jimenez, J. L., Worsnop, D. R., Baltensperger, U., and Prevot, A. S. H.: Inorganic Salt Interference on CO2+ in Aerodyne AMS and ACSM Organic Aerosol Composition Studies, Environ. Sci. Technol., 50, 10494-10503, https://doi.org/10.1021/acs.est.6b01035, 2016.

Qi, L., Chen, M. D., Stefenelli, G., Pospisilova, V., Tong, Y. D., Bertrand, A., Hueglin, C., Ge, X. L., Baltensperger, U., Prevot, A. S. H., and Slowik, J. G.: Organic aerosol source apportionment in Zurich using an extractive electrospray ionization time-of-flight mass spectrometer (EESI-TOF-MS) - Part 2: Biomass burning influences in winter, Atmos. Chem. Phys., 19, 8037-8062, https://doi.org/10.5194/acp-19-8037-2019, 2019.

Stefenelli, G., Pospisilova, V., Lopez-Hilfiker, F. D., Daellenbach, K. R., Hüglin, C., Tong, Y., Baltensperger, U., Prévôt, A. S. H., and Slowik, J. G.: Organic aerosol source apportionment in Zurich using an extractive electrospray ionization time-of-flight mass spectrometer (EESI-TOF-MS) – Part 1: Biogenic influences and day–night chemistry in summer, Atmos. Chem. Phys., 19, 14825-14848, https://doi.org/10.5194/acp-19-14825-2019, 2019.